



Article

Stomatal and Non-Stomatal Leaf Responses during Two Sequential Water Stress Cycles in Young *Coffea canephora* Plants

Danilo F. Baroni ¹, Guilherme A. R. de Souza ¹ , Wallace de P. Bernardo ¹, Anne R. Santos ¹ , Larissa C. de S. Barcellos ¹, Letícia F. T. Barcelos ¹ , Laísa Z. Correia ¹ , Claudio M. de Almeida ¹, Abraão C. Verdin Filho ², Weverton P. Rodrigues ³ , José C. Ramalho ^{4,5} , Miroslava Rakočević ^{1,*} and Eliemar Campostrini ^{1,*}

¹ Setor de Fisiologia Vegetal, Laboratório de Melhoramento Genético Vegetal, Centro de Ciências e Tecnologias Agropecuárias, Universidade Estadual do Norte Fluminense, Avenida Alberto Lamego 2000, Parque Califórnia, Campos dos Goytacazes 28013-602, RJ, Brazil; baronidf@gmail.com (D.F.B.); guilherme.rodrigues@edu.uniube.br (G.A.R.d.S.); wallace-bernardo@hotmail.com (W.d.P.B.); annersantos@outlook.com (A.R.S.); lbarcellos.uenf@gmail.com (L.C.d.S.B.); leticiafbarcelos@gmail.com (L.F.T.B.); laisazanelatocorreia@gmail.com (L.Z.C.); claudio@pq.uenf.br (C.M.d.A.)

² Instituto Capixaba de Pesquisa, Assistência Técnica e Extensão Rural, Vitória 29052-010, ES, Brazil; verdin.incaper@gmail.com

³ Centro de Ciências Agrárias, Universidade Estadual da Região Tocantina do Maranhão, Avenida Agrária 100, Imperatriz, Imperatriz 65900-001, MA, Brazil; weverton.rodrigues@uebrasul.edu.br

⁴ Lab. Interações Planta-Ambiente & Biodiversidade (PlantStress & Biodiversity), Centro de Estudos Florestais (CEF), Laboratório Associado TERRA, Instituto Superior de Agronomia (ISA), Universidade de Lisboa (ULisboa), 1349-017 Lisboa, Portugal; cochichor@mail.telepac.pt

⁵ Unidade de Geobiociências, Geoengenharias e Geotecnologias (GeoBioTec), Faculdade de Ciências Tecnologia, Universidade NOVA de Lisboa, 2829-516 Caparica, Portugal

* Correspondence: mima.rakocevic61@gmail.com (M.R.); campostenator@gmail.com (E.C.)



Citation: Baroni, D.F.; de Souza, G.A.R.; Bernardo, W.d.P.; Santos, A.R.; Barcellos, L.C.d.S.; Barcelos, L.F.T.; Correia, L.Z.; de Almeida, C.M.; Verdin Filho, A.C.; Rodrigues, W.P.; et al. Stomatal and Non-Stomatal Leaf Responses during Two Sequential Water Stress Cycles in Young *Coffea canephora* Plants. *Stresses* **2024**, *4*, 575–597. <https://doi.org/10.3390/stresses4030037>

Academic Editor: Julietta Moustaka

Received: 30 July 2024

Revised: 2 September 2024

Accepted: 3 September 2024

Published: 9 September 2024



Copyright: © 2024 by the authors. Licensee MDPI, Basel, Switzerland. This article is an open access article distributed under the terms and conditions of the Creative Commons Attribution (CC BY) license (<https://creativecommons.org/licenses/by/4.0/>).

Abstract: Understanding the dynamics of physiological changes involved in the acclimation responses of plants after their exposure to repeated cycles of water stress is crucial to selecting resilient genotypes for regions with recurrent drought episodes. Under such background, we tried to respond to questions as: (1) Are there differences in the stomatal-related and non-stomatal responses during water stress cycles in different clones of *Coffea canephora* Pierre ex A. Froehner? (2) Do these *C. canephora* clones show a different response in each of the two sequential water stress events? (3) Is one previous drought stress event sufficient to induce a kind of “memory” in *C. canephora*? Seven-month-old plants of two clones (‘3V’ and ‘A1’, previously characterized as deeper and lesser deep root growth, respectively) were maintained well-watered (WW) or fully withholding the irrigation, inducing soil water stress (WS) until the soil matric water potential (Ψ_{msoil}) reached $\cong -0.5$ MPa (-500 kPa) at a soil depth of 500 mm. Two sequential drought events (drought-1 and drought-2) attained this Ψ_{msoil} after 19 days and were followed by soil rewatering until a complete recovery of leaf net CO_2 assimilation rate (A_{net}) during the recovery-1 and recovery-2 events. The leaf gas exchange, chlorophyll *a* fluorescence, and leaf reflectance parameters were measured in six-day frequency, while the leaf anatomy was examined only at the end of the second drought cycle. In both drought events, the WS plants showed reduction in stomatal conductance and leaf transpiration. The reduction in internal CO_2 diffusion was observed in the second drought cycle, expressed by increased thickness of spongy parenchyma in both clones. Those stomatal and anatomical traits impacted decreasing the A_{net} in both drought events. The ‘3V’ was less influenced by water stress than the ‘A1’ genotype in A_{net} , effective quantum yield in PSII photochemistry, photochemical quenching, linear electron transport rate, and photochemical reflectance index during the drought-1, but during the drought-2 event such an advantage disappeared. Such physiological genotype differences were supported by the medium xylem vessel area diminished only in ‘3V’ under WS. In both drought cycles, the recovery of all observed stomatal and non-stomatal responses was usually complete after 12 days of rewatering. The absence of photochemical impacts, namely in the maximum quantum yield of primary photochemical reactions, photosynthetic performance index, and density of reaction centers

capable of Q_A reduction during the drought-2 event, might result from an acclimation response of the clones to WS. In the second drought cycle, the plants showed some improved responses to stress, suggesting “memory” effects as drought acclimation at a recurrent drought.

Keywords: coffee; fluorescence; gas exchanges; memory effect; parenchyma; xylem vessel area

1. Introduction

Among 130 species in the genus *Coffea* spp. [1], only two are commonly used in commercial coffee production, i.e., *Coffea arabica* L. and *Coffea canephora* Pierre ex A. Froehner. Brazil is the second largest world producer of the latter [2,3], with the small Espírito Santo State, Southeast Brazil, being alone responsible for ca. 15% of the world’s yield [4]. This Brazilian state is characterized by dry winters, demanding irrigation to optimize crop yields [5]. The limitation of water resources for irrigation has increased due to the increment of cropped areas, accompanied by a decline in underground water resources [6], a reduction in rainfall amounts, and their altered temporal distribution, which all have boosted the frequency and severity of drought events sensed by plants in the field [2,7]. Under such reality, the selection of drought-resilient coffee genotypes is of crucial importance to this crop’s sustainability [8].

Plant drought resistance is generally related to four mechanisms [9]: (1) escape from drought [10], (2) drought tolerance [11], (3) drought avoidance [12–17], and (4) drought recovery [18]. It is common to observe a mix of drought tolerance and avoidance mechanisms [9,19] through a combination of morphological, physiological, and anatomical modifications [20] that grant plants the ability to thrive under unfavorable environments.

The drought effects on coffee plants are often observed quickly, even under low to moderate stress levels. Hydraulic conductance and stomatal conductance (g_s) declines prevent excessive water loss. The latter is usually one of the earliest triggered mechanisms to preserve water levels, but it will concomitantly reduce the net CO_2 assimilation rate (A_{net}) [21], limiting biomass accumulation and yield [8]. In fact, mild drought stress can already cause a decrease in photosynthesis in *Coffea* spp. induced by stomatal closure associated with the expression of gene precursors of ABA synthesis [22]. Coffee plants displayed a relatively low A_{net} compared to other C3 species, mainly related to limitations to CO_2 diffusion from the stomata and within mesophyll until carboxylation sites in the chloroplasts, thus associated with low stomatal (g_s) and mesophyll (g_m) conductances [23]. In fact, g_s is the major factor limiting coffee photosynthesis, and such influence is further amplified under drought conditions [24–27]. Under drought, leaf anatomy modifications can additionally occur in *C. arabica*, including the increase in stomatal density and reductions in the adaxial epidermis thickness and in the palisade parenchyma, with a parallel reduction in stomata size [28]. The last can be viewed as a general response related to gas exchange regulation in plants under stress, improving water-use efficiency [29].

Non-stomatal limitations can also occur under drought conditions in various species, demanding acclimation responses at photochemical, biochemical [30–32], and molecular levels. In *Coffea* spp., this includes a number of responses (commonly to several environmental stresses), among them the triggering/reinforcement of protective and antioxidant components associated with transcriptome, proteome, lipidome, and metabolome profiles changes [22,33–37]. Environmental stress impacts can be accessed through in situ and non-destructive measurements, as in the case of the parameters derived from chlorophyll *a* fluorescence (non-stomatal indicators). These indicators can help in the evaluation of the photochemical energy use associated with photosystem II (PSII) activity [38,39], contributing to characterizing the stress impact and the acclimation mechanisms [40–42]. Based on the fast fluorescence kinetics of chlorophyll *a* fluorescence, the OJIP test allows measuring several photochemically related parameters [43–45]. Additionally, chlorophyll *a* fluorescence quenching analysis helps to evaluate PSII photoinhibition and to better understand

the use and dissipation of energy [39,46–49]. As a complementary approach, leaf spectral reflectance is also known to be sensitive to stressor agents [50]. Under a slow-developing drought, pigment contents and ratios will be modified, namely the decrease in chlorophyll content and increase in carotenoid-to-chlorophyll ratio [51]. Those modifications promote significant changes in leaf spectral reflectance in various wavelengths, from visible to short-wavelength infrared regions, which are sensitive to both fast- and slow-developing stresses [51,52].

In the last decade, the knowledge of the mechanisms associated with drought tolerance has grown, although most works addressed the impact of single drought events [53]. The same has been occurring with most stresses being studied as a single occurrence, despite the fact that plants display much more complex impacts and responses to a combination of stresses, not easily extrapolated from single stress events, as reported in *Coffea* spp. [33,37,54]. In a similar way, repeated drought and recovery events are more common than a single sudden or prolonged drought event in natural conditions [55,56]. Thus, some care must be taken to extrapolate information associated with drought responses obtained from a single drought event [53], in particular as regards perennial crops.

Plants, especially under non-irrigated management, are subjected to cycles of drought stress and rewatering across the globe [57]. The processes of the plant repairing the drought-induced damages and restarting the growth are complex, involving the rearrangement of a wide number of metabolic pathways [18]. Therefore, plants can develop some cross-response acclimation when previously exposed to a stress agent, which can potentiate their defense responses for the next stress events and prepare them for a subsequent exposure to that stress agent [33,53,56,58–60]. Still, photosynthesis declines during drought, while the velocity of drought recovery after rewatering and the potential acclimation to subsequent drought cycles have been explored only in a few cases [55]. In *C. arabica* plants grown under field conditions, A_{net} , g_s , leaf transpiration (E), and carboxylation efficiency were similar between irrigated and rainfed conditions only after four recurrent drought periods in all four observed genotypes, suggesting acclimation of leaf gas exchanges at leaf scale [56] or in some architectural traits, such as the individual leaf size [61].

A better understanding of physiological traits and the mechanisms involved in drought acclimation responses provides insights and facilitates the selection of promising *C. canephora* clones for future coffee cropping in drought-prone regions. In this context, some questions were addressed as: (1) Are there differences in the stomatal-related and non-stomatal responses during water stress and recovery events in different clones of *C. canephora*? (2) Do these *C. canephora* clones show a different impact and acclimation response in each of the two consecutive water stress events, expressing a kind of “memory” to the previous event? (3) Is one previous drought stress event sufficient to induce drought acclimation in *C. canephora*? We hypothesized genotype-dependent responses to drought periods, and additionally, that stomatal-related parameters (as A_{net} , g_s , and E) would be less expressive than non-stomatal parameters (as chlorophyll *a* fluorescence, reflectance indexes, and leaf anatomy) in *C. canephora* acclimation to drought during the second drought event.

2. Results

2.1. Soil and Leaf Water Potentials during Two Subsequent Water Stress Cycles

The soil matric water potential (Ψ_{msoil}) gradually decreased in both clones upon irrigation withholding in both drought events (drought-1 and drought-2), and quickly recovered after rewatering (Figure 1). In the pots of ‘3V’ plants, the Ψ_{msoil} at 500 mm depth was lower than at 100 mm by the last, 19th day of drought in both cycles (Figure 2A), contrasting with the soil of ‘A1’, where the lowest Ψ_{msoil} was always found in the 100 mm depth (Figure 2B). Both clones under well-watered (WW, control) conditions showed $\Psi_{\text{msoil}} > -12$ kPa (-0.012 MPa).

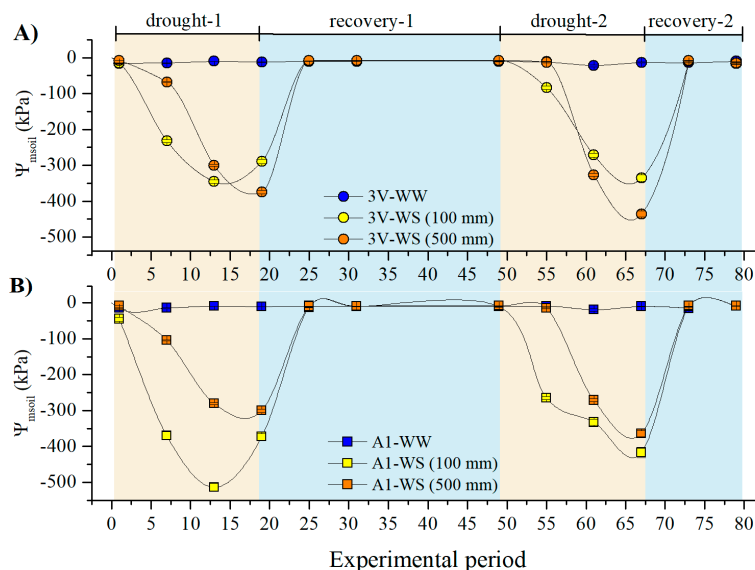


Figure 1. Soil matric water potential (Ψ_{msoil}) at 100 mm cm and 500 mm from the soil surface in the pots of the *C. canephora* var. Robusta genotypes of (A) ‘3V’ and (B) ‘A1’ under well-watered (WW) and water stressed (WS) conditions. The water restriction was imposed during the drought-1 and drought-2 events, after which the soil was rewatered (and recovery-1 and recovery-2 events).

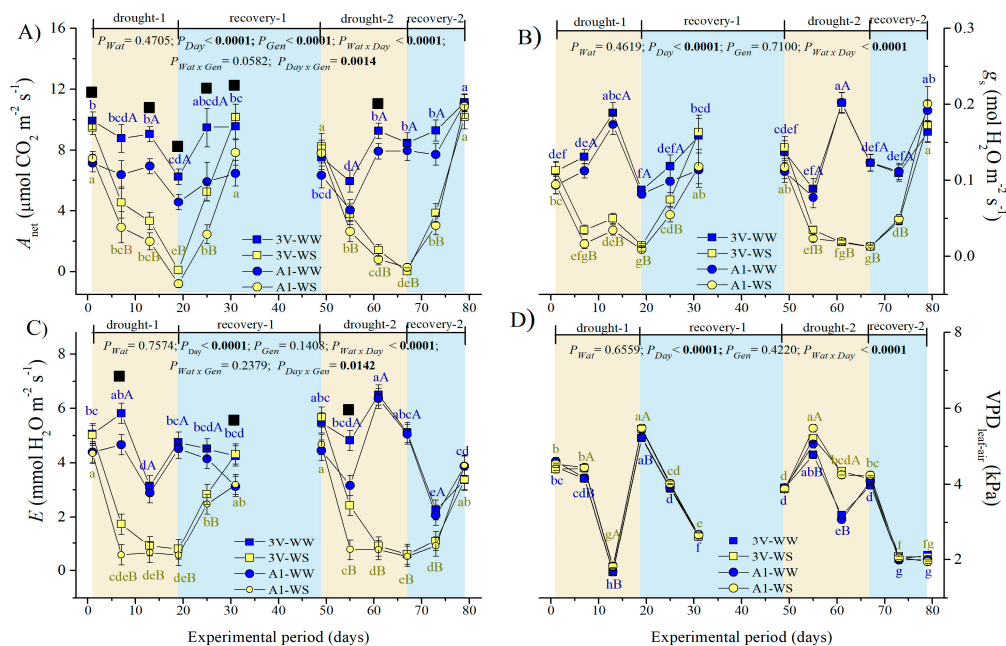


Figure 2. Leaf gas exchanges of two genotypes (Gen) of *C. canephora* var. Robusta (‘3V’ and ‘A1’) grown under two water availability conditions [Wat, well-watered (WW) and water stress (WS)], over 12 time-points of six-day intervals (Day) during drought-1 and drought-2 and respective recovery events: (A) net CO₂ assimilation rate (A_{net}), (B) stomatal conductance to water (g_s), (C) transpiration rate (E), and (D) leaf-to-air vapor pressure deficit ($VPD_{\text{leaf-air}}$). Inside the figures, the different lowercase letters indicate the significant difference among the time-points for each water regime (blue for WW and olive green for WS); different uppercase letters indicate the comparison between water availabilities for each time-point of observation (blue for WW and olive green for WS); and different superscript black ■ signs indicate that ‘3V’ was statistically superior to ‘A1’ at that time-point. Mean \pm SE and ANOVA p -values ($n = 7$) for effects of three factors (water availability, genotype, and day of observation) and their interactions are shown. The significant p -values were marked in bold in the upper part of each graph.

Leaf water potential (Ψ_{leaf}) of plants grown under water stress differed among drought cycles only in the '3V' clone, attaining more negative values in the drought-2 than drought-1 cycle at predawn of the first day of recovery (Table S1). The Ψ_{leaf} had significantly lower values in WS than in WW plants of both genotypes, but no difference was observed between the genotypes within each type of water availability condition in none of the cycles.

2.2. Leaf Gas Exchanges during Two Subsequent Water Stress Cycles

The A_{net} of WW plants kept certain stability over time, with values between 5 and 7 $\mu\text{mol m}^{-2} \text{s}^{-1}$ and between 7 and 10 $\mu\text{mol m}^{-2} \text{s}^{-1}$ in '3V' and 'A1', respectively, during the drought-1 and drought-2 events (Figure 2A). In sharp contrast, regardless of genotype, the WS plants showed a drastic A_{net} reduction down to $\sim 0 \mu\text{mol m}^{-2} \text{s}^{-1}$ by the end of both drought events and a declining pattern similar in both cycles. A similar pattern was also found in A_{net} recovery for both genotypes and drought cycles. The only difference between the drought-1 and drought-2 events was observed in genotype sensitivity to drought, approaching A_{net} values of 'A1' to '3V' during the drought-2, while the A_{net} values of '3V' were continuously superior to 'A1' during the drought-1 and recovery-1 events.

Stomatal conductance increased significantly after 12 days under control (WW) in both drought events and in both clones (Figure 2B). In other time points, g_s was near the initial value, permitting maintaining the A_{net} at a similar level as the initial value in each drought event (Figure 2A). Under the WS conditions, the drastic g_s reduction occurred in both drought events to similar values, as happened with g_s recovery dynamics (Figure 2B). A complete g_s recovery was achieved after rewatering similarly for both cycles and genotypes.

Leaf transpiration rate (E) decreased significantly after 12 days under control (WW) in the drought-1 event compared to the initial value in both clones (Figure 2C), contrary to the mentioned g_s variation (Figure 2B). Under the WS conditions, a drastic E reduction occurred already by the seventh day and onwards, similar in both drought cycles, whereas a slighter recuperation was observed at recovery-2 than at recovery-1, by comparing significant differences between the values of the first time-point of each cycle in recovery dynamics (Figure 2C). The complete E recovery was achieved after rewatering that followed both drought events. The dynamics in E were similar between the two genotypes, but E was higher in '3V' than in 'A1' at the seventh day of both drought events.

The leaf-to-air vapor pressure deficit ($\text{VPD}_{\text{leaf-air}}$) decreased drastically after 12 days under both WW and WS conditions in the drought-1 event compared to the initial values of both clones (Figure 2D), similar to what happened to E (Figure 2C), which seemed to be induced by decreased air temperature (Figure S1B) and increased air RH (Figure S1C), due to rains. Under the WS conditions, the significant $\text{VPD}_{\text{leaf-air}}$ increase was observed in both drought events compared to WW conditions, but it was significantly higher during drought-2 than during drought-1 event (Figure 2D), indicating either drought acclimatization or consequence of external climate conditions (Figure S1). The complete $\text{VPD}_{\text{leaf-air}}$ recovery was achieved by the end of each of the two cycles (Figure 2D). The $\text{VPD}_{\text{leaf-air}}$ attained lower values at the end of recovery-2 than at the recovery-1 event, again indicating either acclimatization to drought or external air condition impacts. The dynamics in $\text{VPD}_{\text{leaf-air}}$ were similar between the two genotypes.

The highest values of water-use efficiency (WUE) were observed at the seventh day of the drought-1 under WS, differing significantly when compared to WW conditions (Figure 3). At the end of the drought-1 and drought-2 events, the WUE in plants grown under WS fell to the lowest values, due to negligible A_{net} values (Figure 2A). The WUE recovered at the end of each cycle, being the highest in the recovery-2 event (Figure 3). No genotype-dependent effect was observed on WUE during the two drought cycles.

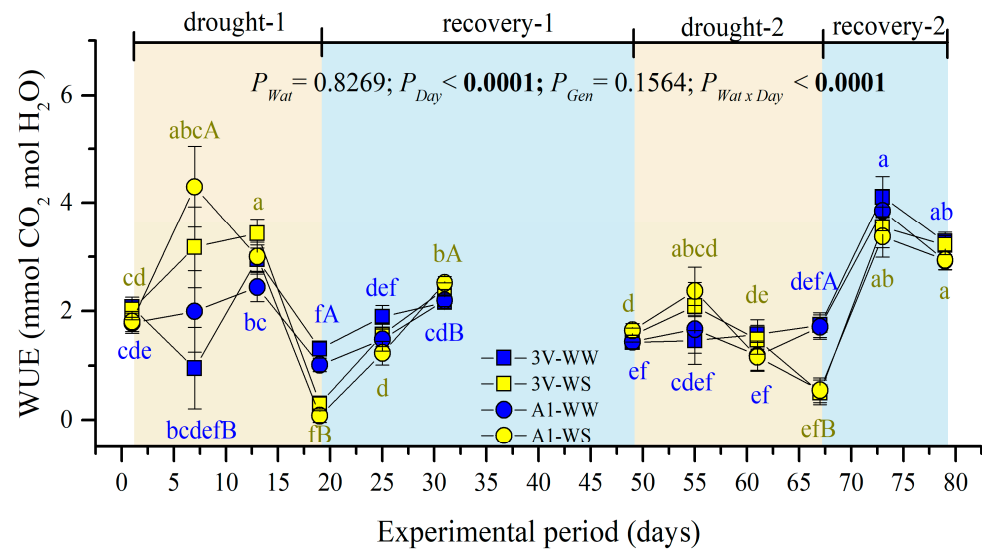


Figure 3. Instantaneous water-use efficiency (WUE, A_{net}/E) of two genotypes (Gen) of *C. canephora* var. Robusta ('3V' and 'A1') grown under two water availability conditions [Wat, well-watered (WW) and water stress (WS)], over 12 time-points of six-day intervals (Day) during drought-1 and drought-2 and respective recovery events. Inside the figure, different lowercase letters indicate the significant difference among the day-time points for each water regime (blue for WW and olive green for WS); different uppercase letters indicate the comparison between water availabilities for each time-point of observation (blue for WW and olive green for WS). Mean \pm SE and ANOVA p -values ($n = 7$) for effects of three factors (water availability, genotype, and day of observation) and their interactions are shown. The significant p -values were marked in bold in the upper part of each graph.

2.3. Leaf Chlorophyll *a* Fluorescence during Two Subsequent Water Stress Cycles

2.3.1. Dynamics of Non-Modulated Fluorescence

The maximum quantum yield of primary photochemical reactions (ΦP_0), probability of electron transfer from the Q_A - to electron transport chain beyond Q_A (ΨE_0), photosynthetic performance index (PI_{ABS}), and density of reaction centers capable of Q_A reduction RC/CS_0 of WW plants were moderately stable over the experimental period (Figure 4). Additionally, ΦP_0 did not significantly change in WS plants in the drought-1 event compared to the initial value (Figure 4A). A significant decline of ΦP_0 was observed at the end of the drought-2 event, although it displayed a similar value to one found at the comparable time-point in the first cycle. The difference between WW counterparts was relatively small in the second recovery event. Still in WS plants, the ΦP_0 did not fully recover at the end of both recovery events, as compared with their respective WW plants at the same time-points. Significant differences in ΦP_0 between the WW and WS plants were observed at the 13th, 19th (drought-1), 31st (recovery-1), 73rd, and 79th (recovery-2) days of the experiment, while the genotype effect on ΦP_0 was not observed. Notably, the ΦP_0 parameter seems to be less impacted by drought during the second than in the first drought event (except at the harshest drought point, the 19th day of each cycle).

The ΨE_0 fluctuated in WS plants of both clones and drought events (Figure 4B). The significant decrease in ΨE_0 was achieved at the 19th day of water withdrawal in both drought events. The complete ΨE_0 recovery in WS plants was achieved in recovery-1 but not in recovery-2 events in both genotypes. Curiously, something similar in ΨE_0 also happened with WW plants in the recovery-2 event. ΨE_0 values were significantly higher in drought-2 than in drought-1 event, comparing all time-points of drought-exposed plants, occurring similarly in WS and WW plants, last indicating some kind of acclimation in the second drought cycle. The ΨE_0 of 'A1' was more impacted by drought than '3V' at the end of the drought-1 event. '3V' also showed higher ΨE_0 values than 'A1' at the beginning of the drought-2 event.

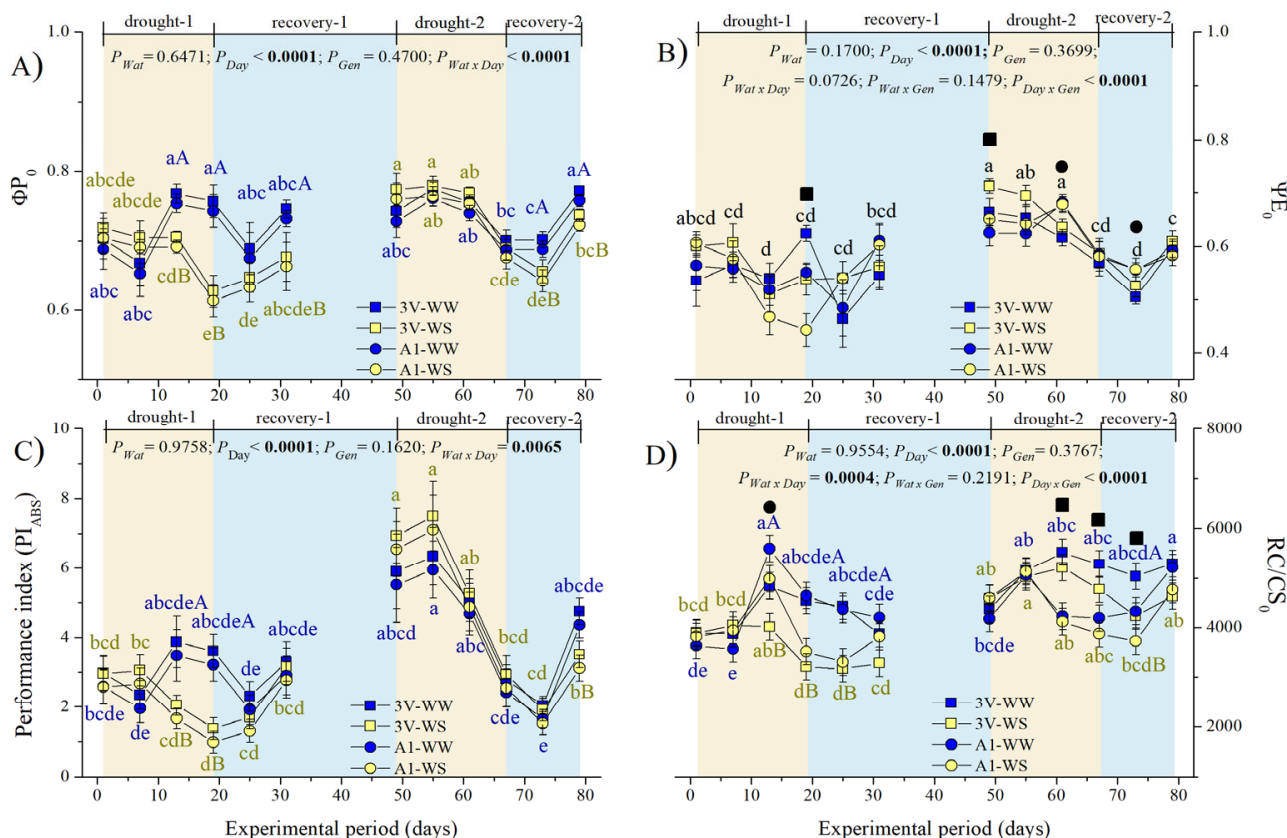


Figure 4. Variation of OJIP indexes of two genotypes (Gen) of *C. canephora* var. Robusta ('3V' and 'A1') grown under two water availability conditions [Wat, well-watered (WW) and water stress (WS)] over 12 time-points of six-day intervals (Day) during drought-1 and drought-2 and respective recovery events: (A) maximum quantum yield of primary photochemical reactions (ΦP_0), (B) probability of electron transfer from Q_A -to-electron transport chain beyond Q_A (ΨE_0), (C) photosynthetic performance index (PI_{ABS}), and (D) density of reaction centers capable of Q_A reduction (RC/CS_0). Inside the figures, the different lowercase letters indicate the significant difference among the time-points for each water regime (blue for WW and olive green for WS); different uppercase letters indicate the comparison between water availabilities for each day of observation (blue for WW and olive green for WS); superscript black ■ signs indicate that '3V' was statistically superior to 'A1', while superscript black ● signs indicate that 'A1' clone was statistically superior to '3V' clone at that time-point. Mean \pm SE and ANOVA P -values ($n = 7$) for effects of three factors (water availability, genotype, and day of observation) and their interactions are shown. The significant P -values were marked in bold.

The photosynthetic performance index (PI_{ABS}) was generally higher during the drought-2 and at the end of recovery-2 as compared to corresponding points during the first cycle, both for WW and WS plants (Figure 4C). At the 13th and 19th days of the drought-1 event, the PI_{ABS} values were significantly higher in WW than in WS plants, while no difference between the WW and WS plants was observed in the second cycle, indicating a drought acclimation in the second drought event, although the WS plants denoted an incomplete recovery by the end of the second cycle but not by the end of the first one.

2.3.2. Dynamics of Modulated Chlorophyll *a* Fluorescence

The absolute values of modulated leaf chlorophyll *a* fluorescence parameters: effective quantum yield in PSII photochemistry (Φ_{PSII}), photochemical quenching (qP), non-photochemical quenching (NPQ), and linear electron transport rate (ETR) in WW plants showed a certain fluctuation over time, even in WW plants (Figure 5). The Φ_{PSII} , qP , and ETR decreased in the WS-exposed plants in both clones and cycles (Figure 5A,B,D). The maximum decline of those parameters (ca. 70–80%) was observed by the harshest drought

conditions just before rewatering (19th day and 67th day of the first and second cycles). The drop in Φ_{PSII} , qP , and ETR values was similar between the two drought cycles. Such reduction in Φ_{PSII} , qP , and ETR of WS plants was greater in 'A1' than '3V' only in the first cycle, while no difference between '3V' and 'A1' was found during the second cycle, indicating that 'A1' clone drought sensitivity diminished in cycle 2. The complete recovery of those three Chl *a* fluorescence parameters was found by the end of both recovery events.

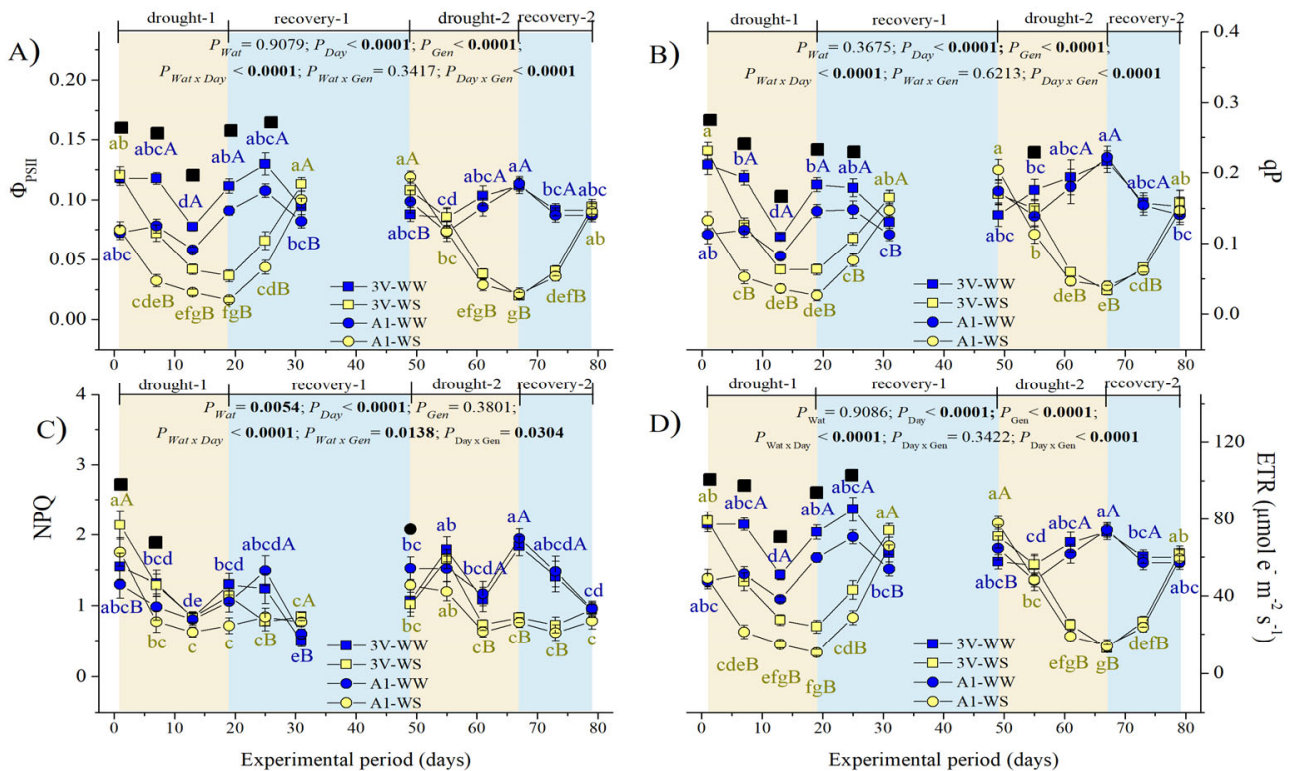


Figure 5. Variation of modulated chlorophyll *a* fluorescence indexes of two genotypes (Gen) of *C. canephora* var. Robusta ('3V' and 'A1') grown under two water availability conditions [Wat, well-watered (WW) and water stress (WS)] over 12 time-points of six-day intervals (Day) during drought-1 and drought-2 and respective recovery events: (A) effective quantum yield in PSII photochemistry (Φ_{PSII}), (B) photochemical quenching (qP), (C) non-photochemical quenching (NPQ), and (D) linear electron transport rate (ETR). Inside the figures, the different lowercase letters indicate the significant difference among the time-points for each water regime (blue for WW and olive green for WS); different uppercase letters indicate the comparison between water availabilities for each day of observation (blue for WW and olive green for WS); different superscript black ■ signs indicate that '3V' was statistically superior to 'A1', while superscript black ● signs indicate that 'A1' clone was statistically superior to '3V' clone at that time-point. Mean \pm SE and ANOVA *p*-values ($n = 7$) for effects of three factors (water availability, genotype, and day of observation) and their interactions are shown. The significant *p*-values were marked in bold.

The NPQ values dropped significantly in WW and WS plants during the first cycle, denoting low values by the end of the recovery-1 event, close to WW and WS plants in both genotypes (Figure 5C). Still, unexpectedly, NPQ tended to their lowest values in WS plants of 'A1' in the first cycle and both genotypes in the second cycle, thus denoting a reduction in thermal dissipation energy processes upon drought exposure.

2.4. Spectral Reflectance Indices of Leaf Adaxial Surface during Two Subsequent Water Stress Cycles

The leaf green chlorophyll index (GCI) did not significantly change in WW plants within each cycle (Figure 6A). During the drought-2 event, higher GCI values were observed

in WW than in WS plants at 55th day, with inversion at 61st day (higher in WS than in WW plants) indicating chlorophyll reduction under drought at those time-points, while during the recovery-2 event, no water stress effect was observed in GCI. At the initial time-point of drought-1, initial of recovery-1 and recovery-2 events, the GCI was higher in '3V' than in 'A1' clone, indicating that '3V' clone had more chlorophyll irrespective of water conditions.

There was no effect of drought on carotenoid reflectance index (CRI) in any of the genotypes in the first and second drought cycles since the CRI variations occurred in parallel (and with similar values) in WW and WS plants (Figure 6B). CRI varied significantly over the time, being dependent only on genotype and being significantly lower in the second than in the first drought cycle. It was higher in '3V' than in 'A1' at the beginning and at the end of both drought events, as a general genotype characteristic of higher carotenoid content of '3V' clone, irrespective of water conditions. The 'A1' showed higher CRI than '3V' at the 19th day in the harshest moment of the drought-1 event, but not differing among the WW and WS plants, while during the recovery-1, the CRI was recovered, being again higher in '3V' than in 'A1' leaves.

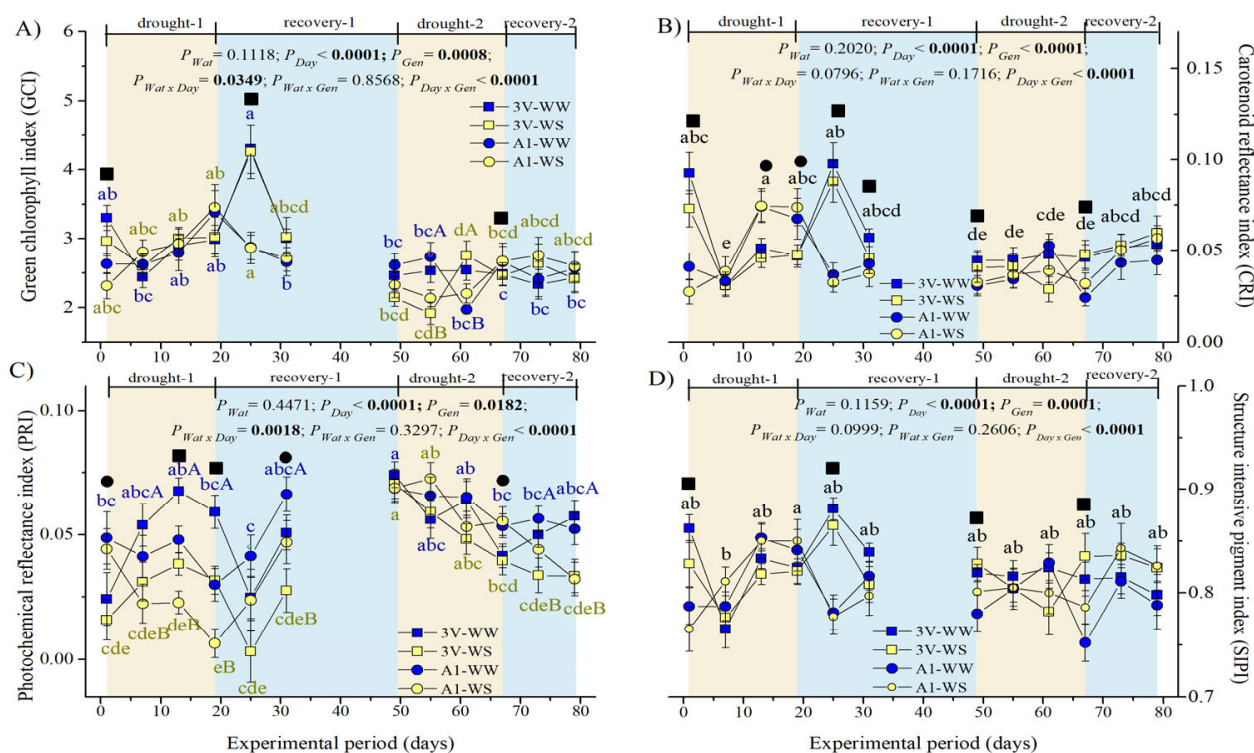


Figure 6. Variation of spectral reflectance indices of leaf adaxial surface of two genotypes (Gen) of *C. canephora* var. Robusta ('3V' and 'A1') grown under two water availability conditions [Wat, well-watered (WW) and water stress (WS)] over 12 time-points of six-day intervals (Day) during drought-1 and drought-2 and respective recovery events: (A) green chlorophyll index (GCI), (B) carotenoid reflectance index (CRI), (C) photochemical reflectance index (PRI), and (D) structure intensive reflectance index (SIPI). Inside the figures, the different lowercase letters indicate the significant difference among the time-points for each water regime (blue for WW and olive green for WS); different uppercase letters indicate the comparison between water availabilities for each day of observation (blue for WW and olive green for WS); different superscript black ■ signs indicate that '3V' was statistically superior to 'A1', while superscript black ● signs indicate that 'A1' clone was statistically superior to '3V' clone at that time-point. Mean \pm SE and ANOVA p -values ($n = 7$) for effects of three factors (water availability, genotype, and day of observation) and their interactions are shown. The significant p -values were marked in bold.

The photochemical reflectance index (PRI) maintained higher values in WW plants than in WS counterparts in most parts of both cycles, but with a greater difference in the

first cycle (Figure 6C). In the second drought cycle, the PRI values of WS plants were significantly higher than in the first drought cycle, and the values of WS plants were closer to those of WW plants (when they were in the first cycle), suggesting acclimation. By the end of the recovery periods, no differences were observed between cycles. During the drought-1 and recovery-1 events, the PRI values of '3V' were superior to 'A1', while no clonal difference was observed during the second cycle, indicating the loss of greater 'A1' sensitivity.

The structure-intensive reflectance index (SIPI) values varied over the time due to genotype, irrespective of water stress (Figure 6D). The '3V' showed higher SIPI than 'A1' at the beginning of drought-1, recovery-1, and drought-2 time-points, and at the end of the drought-2 event, as an additional index of higher chlorophyll content of '3V' than 'A1' clone (Figure 6A). The lowest SIPI values were observed at the seventh day of drought imposition and the highest at the end of the drought-1 event (Figure 6D).

2.5. Leaf Anatomy after Two Drought Cycles

Stomatal density was genotype-dependent, showing greater values in '3V' than in 'A1' clone, irrespective of water availability conditions (Table 1).

Table 1. Leaf anatomy parameters evaluated at the end of the second drought cycle of *Coffea canephora* var. Robusta clones ('3V' and 'A1') are grown under well-watered (WW) and water stress (WS) conditions.

Leaf Anatomy Parameter	Well-Watered (WW)		Water-Stress (WS)		p-Value		
	'3V'	'A1'	'3V'	'A1'	Clone	Water	Interaction
Stomatal density (number stomata mm ⁻²)	269.5 ± 8.7 aA	251.5 ± 6.9 bA	278.0 ± 18.2 aA	250.7 ± 7.5 bA	0.0370	0.8920	-
Leaf thickness (µm)	221.7 ± 3.0 bA	228.6 ± 3.6 aB	221.7 ± 3.7 bA	241.3 ± 2.6 aA	<0.0001	0.0420	0.0500
Thickness of adaxial epidermis (µm)	21.07 ± 0.6 aA	20.87 ± 0.5 aA	20.4 ± 0.4 aA	21.1 ± 0.6 aA	0.4810	0.6530	-
Thickness of abaxial epidermis (µm)	14.0 ± 0.4 aA	13.7 ± 0.5 aA	13.4 ± 0.3 aA	13.9 ± 0.3 aA	0.6020	0.4930	-
Thickness of palisade parenchyma (µm)	54.0 ± 1.6 aA	48.6 ± 0.9 bA	46.6 ± 1.4 aB	46.2 ± 3.0 aA	0.2980	0.0020	0.0191
Thickness of spongy parenchyma (µm)	131.4 ± 3.4 bB	147.3 ± 3.8 aB	140.7 ± 3.5 bA	158.7 ± 3.7aA	<0.0001	0.0070	-
Density of xylem vessels (number * 10 ⁻⁵ µm ⁻²)	172.1 ± 9.2 aA	190.2 ± 10.5 aA	188.4 ± 11.1 aA	182.5 ± 7.7 aA	0.2430	0.8570	-
Medium area of xylem vessel (µm ²)	234.1 ± 9.5 aA	203.6 ± 11.3 bA	190.0 ± 11.0 aB	200.0 ± 9.7 aA	0.2050	0.0370	0.0476

Mean ± SE and P-values (n = 7) for effects of genotype and water availability conditions are shown; $p \leq 0.05$ is highlighted in bold. Lower-case letters indicate significant differences between clones in each water condition; different upper-case letters indicate significant differences between water conditions within each clone.

Leaf thickness changes were associated with genotype characteristics. The 'A1' clone had higher leaf thickness than the '3V' clone under both water conditions, and 'A1' leaf thickness additionally increased under WS conditions (Table 1). The '3V' clone did not change the leaf thickness under the studied water stress conditions, indicating that it was less sensitive to drought between the two studied genotypes, based on total leaf thickness. The thickness of abaxial and adaxial epidermis was irresponsive to water conditions and did not differ between the two clones. The palisade parenchyma thickness was significantly higher in '3V' than in 'A1' under the WW, but not in WS plants, due to a decline of their value in '3V'-WS plants, whereas 'A1' value was irresponsive to water availability. The increased leaf thickness in 'A1'-WS plants compared to 'A1'-WW was mostly related to an increase in spongy parenchyma thickness. Spongy parenchyma thickness was also larger in 'A1' than in '3V' genotype under both water conditions and increased under the WS in both clones.

The xylem vessel density did not differ between the two clones or water availabilities (Table 1), but the medium area of a xylem vessel was larger in '3V' than in 'A1' in

WW condition (Figure 7), decreasing in '3V'-WS plants but not in 'A1'-WS ones, the last irresponsive to water conditions (Table 1).

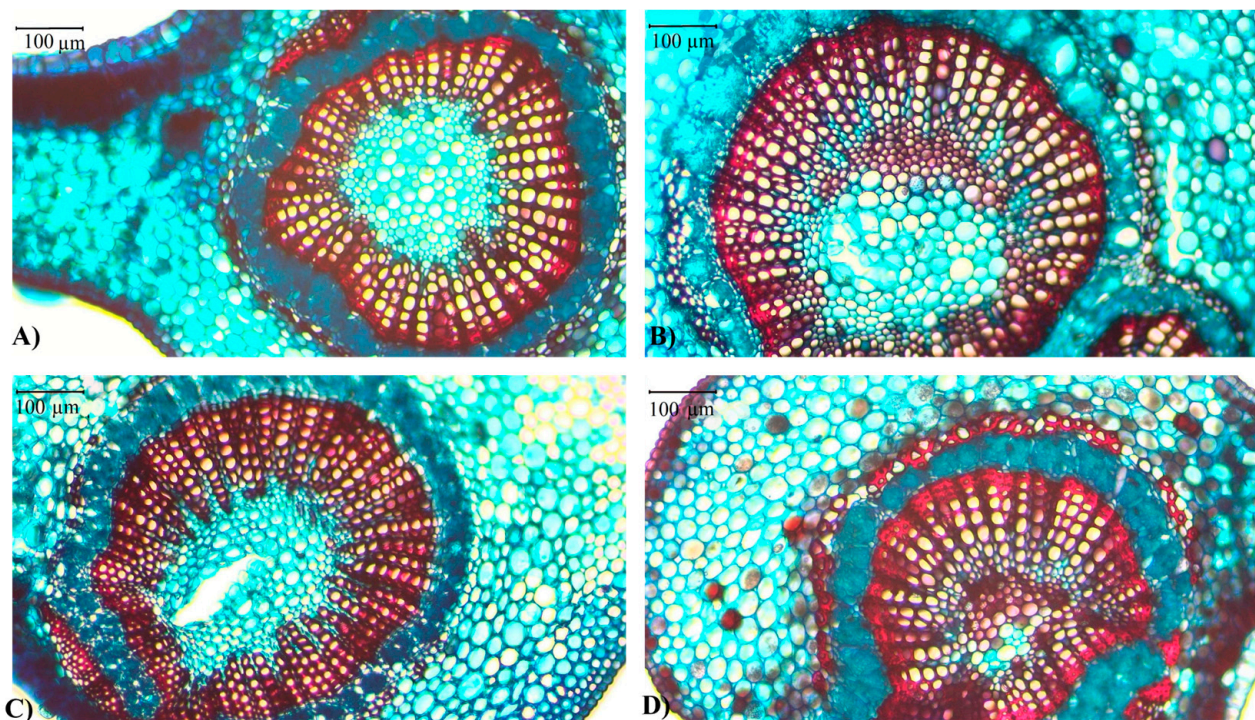


Figure 7. Representative area of leaf xylem vessel (μm^2) measured in *C. canephora* var. Robusta clones ('3V' and 'A1') under well-watered (WW) and water stress (WS) conditions: (A) A1-WW, (B) 3V-WW, (C) A1-WS, and (D) 3V-WS, evaluated at the end of the second drought cycle. A scale of 100 μm is shown.

3. Discussion

The characterization of physiological responses to two subsequent water stress events in *C. canephora* provided insights related to drought tolerance (and acclimation) in a second cycle of drought. This acclimation was especially related to the loss of drought sensitivity during the drought-2 event previously expressed in the 'A1' genotype during the drought-1. Which were the physiological traits that supported such a statement? As expected, drought stress reduced A_{net} (Figure 2A), which was associated with stomatal limitations to great extent in both water stress events (Figure 2B), but stomatal-related responses did not show acclimation in the second compared to the first drought cycle (Figure 2). On the other hand, some non-stomatal responses, even after only one previous drought event, indicated some fine-tuning genotype-specific acclimation, as observed in some chlorophyll *a* fluorescence parameters (Figures 4 and 5) and leaf anatomical regulations (Table 1). In both drought cycles, both clones denoted a quick stomatal response (Figure 2B) to soil water limitation (evaluated through the Ψ_{msoil} , Figure 1) in order to control additional water loss, avoiding/delaying excessive drop in a xylem pressure, as a mechanism involved in protecting xylem from catastrophic hydraulic failure [62–65]. Under water stress conditions occurred the reduction of g_s (Figure 2B), which is limiting CO_2 diffusion into the leaves [66]. Here, increased thickness of spongy parenchyma (Table 1), which can additionally reduce carbon flow and reduce C-assimilation by RuBisCO by lowering CO_2 availability at carboxylation sites [67], contributed to the observed decline of A_{net} (Figure 2A). Also, under the WS, the medium xylem vessel area diminished only in '3V', as a kind of anatomical response to these stress conditions, which is reported to contribute to preserving the water column and avoiding cavitation [3,68].

The A_{net} reduction under water stress was also accompanied by impacts in other non-stomatal parameters. For example, the decline of ΦP_0 during the drought-1 might indicate a certain degree of photoinhibition under WS (Figure 4A), often associated with an overproduction of reactive oxygen species, due to the excessive reduction in plastoquinone Q_A or the charge recombination between the acceptor and donor sides of PSII [69,70]. To better understand this response, we examined what happened to Φ_{PSII} [71]. This parameter (Figure 5A) reinforced the possibility of photoinhibition occurrence associated with a parallel decrease of decrease in PRI (Figure 6C), which constantly maintained lower values under WS than under WW conditions, during both drought and recovery events, indicating reduced light use efficiency in WS plants, but without chlorophyll degradation, discerning based on GCI and SIPI, which were stable over the time (Figure 6A and 6D, respectively). The photoinhibition can also be related to decreases in Φ_{PSII} and ETR (Figure 5A and 5D, respectively) in both genotypes. Higher sensibility of 'A1' than in '3V' expressed in Φ_{PSII} , ETR, and qP disappeared in the second cycle, indicating a kind of genotype-dependent response to drought.

As expected, qP (Figure 5B) showed the same trend as Φ_{PSII} and ETR in both clones during the two water stress events. However, there was a non-significant trend towards modifications of NPQ with the increase of the drought severity, contrary to what might be expected (Figure 5C). In fact, NPQ is related to the thermal dissipation of the excess of absorbed energy [71], usually linked to the xanthophyll cycle [72], and is usually found to increase as the photochemical use of energy (through photosynthesis) is reduced, as was the case here. Additionally, the PRI also declined. This index reflects the de-epoxidation state of the xanthophyll cycle and is strongly correlated with NPQ, being a good indicator of plant stress status in remote sensing [73]. The xanthophyll cycle is strongly related to higher PRI and NPQ values, i.e., greater is the cycle activity, higher are NPQ and PRI values. In our experiment, the xanthophyll cycle was not activated as a stress protection since NPQ and PRI values declined, thus did not grant the plants an additional control of reactive oxygen species [71]. In the xanthophyll cycle, violaxanthin is converted to zeaxanthin when exposed to light excess [74–76]. Zeaxanthin is considered the last product in carotenoid hydroxylases, integrally or peripherally associated with chloroplast membranes [77]. In our experiment, the carotenoid reflectance index (CRI) was genotype dependent but did not vary due to water stress events (Figure 6A). Carotenoid contents tend to decrease under moderate drought but increase slightly under severe drought stress [78]. Therefore, our results indicated that no production of carotenoids was triggered by our experimental drought intensity and duration.

At the 19th day of water withdrawal in both drought events (short-term strong water stress), the WUE was higher in WW than in WS plants in both genotypes, which was a consequence of the negligible A_{net} values (more than the very low g_s ones) (Figure 3). The stomatal control of water loss (that also limits CO_2 access to the carboxylation sites) is one of the traits characterizing drought-tolerant coffee plants [8,79,80], here not differing between the two studied genotypes. Such control was very quick, since by the second time-point (seventh day of each cycle) in both cycles, g_s values reached values close to their minimum (found at the 19th day after suspending irrigation in both cycles). Notably, by the seventh day of each cycle, the A_{net} was already significantly decreased compared to the initial value, and these A_{net} values continued to decline despite the fact that g_s was not further significantly reduced, thus suggesting a gradual increase in non-stomatal limitations to C-assimilation as drought becomes more severe, similarly in both genotypes and in both cycles. Such growing non-stomatal limitations by the 19th day of each cycle agree with (and are reflected by) the decline of several fluorescence parameters, as ΦP_0 , ΨE_0 , RC/CS_0 (clearer in the first cycle) and Φ_{PSII} , qP, and ETR (in both cycles). However, it is noteworthy that by the end of the recovery periods, all these stomatal and non-stomatal parameters showed complete (or close to) recoveries as compared with their WW plants at the same moment.

Plant water status and photosynthetic performance are directly/indirectly associated with the whole plant hydraulic conductivity through the soil–root–shoot–leaf continuum [81]. Therefore, the absence of photochemical impacts of ΦP_0 , PI_{ABS} , and RC/CS_0 during the drought-2 event (as compared to WS and WW plants at each point of that cycle) might have resulted from an acclimation response of the clones, promoted by the previous drought exposure (first cycle) and modulated by hydraulic and anatomic adjustments, as well as a medium area of xylem vessel and spongy parenchymal thickness (Table 1).

Stress “memory” depends on the intensity of the priming event as well as on genetic characteristics that influence stress tolerance [82]. The recovery time of the water deficit is fundamental and can be considered a major component of drought tolerance [9]. In our experiment, this recovery differed between the two genotypes in the first drought cycles but showed similar dynamics in the second drought cycle. When the plants of drought-sensitive clones of *C. canephora* are exposed to multiple water deficit episodes in greenhouses, they may trigger an oxidative stress response, while in tolerant plants, the acclimation involves antioxidant secondary metabolism and the ABA response [83]. This indicates that both here studied genotypes developed acclimation responses and can be considered drought-tolerant. A different situation is observed under field conditions, where soil might buffer the negative impacts of water deficits together with a developed root system of adult plants, impacting on time regarding acclimation responses, where the acclimation in *C. arabica* is reported only after one year and a half, after passing through four drought cycles [56].

The analyses of stomatal and non-stomatal physiological leaf responses indicated that two repeated drought stress periods in glasshouse helped to segregate only the response in PI_{ABS} , but still not attaining profoundly the chlorophyll content (PRI and GCI indexes), but eventually promoting the protective systems, probably via reinforcement of the antioxidant system, as observed in several single and combined stress conditions, including drought [33,37,39].

As concluding remarks, the soil water stress caused a negative impact on plant physiological performance in both stomatal and non-stomatal parameters, observed in both clones of *C. canephora* studied. Under the soil water stress, the reduction of g_s (and E) and of internal CO_2 diffusion occurred, the last here expressed by increased thickness of spongy parenchyma (evaluated at the end of the second cycle) in both clones. Those stomatal and anatomical traits impacted decreased A_{net} . The ‘3V’ was less influenced by water stress than ‘A1’ in some physiological parameters (A_{net} , Φ_{PSII} , qP , ETR, and PRI) during the drought-1, but this response of higher ‘3V’ drought tolerance was lost during the drought-2 event. Physiological genotype differences were supported by the medium xylem vessel area diminished only in ‘3V’ plants grown under water stress. The absence of photochemical impacts of ΦP_0 , PI_{ABS} , and RC/CS_0 (non-stomatal responses) during the drought-2 event might be a result of an acclimation response of the clones to water stress conditions. These findings confirmed our initial hypothesis, i.e., some of the non-stomatal-related parameters were associated with acclimation to drought in *C. canephora* during the second drought event to a greater extent. In fact, photochemical and anatomic adjustments were more determinant in the acclimation process to two repeated water stress events than stomatal adjustments. Therefore, non-stomatal traits should be considered in coffee breeding programs that aim to release new well-adapted cultivars for a changing climate. Despite various indicators of acclimations to water stress in the second drought cycle, it seems that more than two drought cycles could bring stronger acclimation of both stomatal and non-stomatal parameters to drought, especially in the latter, as observed in plant “memory” of the field-cultivated coffee plants.

4. Materials and Methods

4.1. Experimental Conditions

The experiment was carried out in the greenhouse at the State University of Northern Rio de Janeiro, Campos dos Goytacazes (21°44′47″ S and 41°18′24″ W, 10 m altitude), RJ, Brazil, using plants from two clones of *C. canephora* Pierre ex Froehner variety Robusta with

contrasting root growth, '3V' and 'A1' (July 2020, 'Instituto Capixaba de Pesquisa', 20,271° S and 40,306° W, 9 m a.l., Vitória ES, Brazil), previously characterized as deeper and lesser deep root growth, respectively, in 17-month-old plants grown under non-limited water conditions [84]. The roots had grown without depth limitations, as verified by opening and closing the 'holes' in the tubes during the experiment and by examining the substrate from the tubes at the end of the experiment. In November 2020, five-month-old seedlings (14 of each clone) produced from cuttings were transplanted to PVC tubes (1.0 m height × 0.2 m diameter). Tubes were filled with substrate composed of red–yellow latosol and sand (4:1 proportion). Soil chemical analysis was performed to determine the soil fertility and ensure adequate fertilization according to crop requirements [85]. Soil pH determined in H₂O was 5.6, effective cation exchange capacity = 4.0 cmol_c dm⁻³, basis saturation 78.3% (Table S2). The concentration of P, K, Fe, Cu, Zn, Mn, S, and B was 25.5, 372, 25.5, 0.4, 6.4, 27.6, 429.4, and 6.8 mg dm⁻³, respectively, while that of Ca, Mg, Al, H+Al, and Na was 1.1, 1.7, 0.0, 1.1, and 0.2 cmol_c dm⁻³, respectively. The C and organic matter concentrations were 0.6 and 1%.

4.1.1. Micrometeorological Measurements

The micrometeorological variables, such as air temperature (T_{air} , °C), relative humidity (RH, %), air vapor pressure deficit (VPD_{air}, kPa), and photosynthetic photon flux density (PPFD, $\mu\text{mol m}^{-2} \text{s}^{-1}$), were recorded each 60 min from 7 a.m. to 6 p.m., every day, using a Weather Station Watchdog 2000 (Spectrum Technologies, Plainfield, IL, USA), placed inside the greenhouse, close to the plants used in the experiment.

The environmental parameters inside the greenhouse showed variation along the experiment, with low and maximum values of photosynthetic active radiation (PPFD) and T_{air} (and opposite of air relative humidity (RH) and air vapor pressure deficit (VPD_{air})) associated with cloudy and sunny days, respectively, but keeping in a general context a similar condition from the beginning until the end of the experiment (Figure S1).

4.1.2. Plant Watering Conditions and Water Deficit Implementation

Soil was watered daily to maintain full water availability during the first 60 days after transplanting. On the 60th day after transplanting, the plant roots were ca. 300 mm deep (observed by 'holes' in the tubes). After this period, at the end of January 2021, seven plants per clone were exposed to water stress (WS), while the remaining seven plants were maintained under well-watered conditions (WW, control). Soil matric water potential (Ψ_{msoil}) was uninterruptedly recorded each 30 min until the end of the experiment (20 April 2021), using a TEROS 21, Ψ_{msoil} sensor together with a data logger (ZL6 PRO, Meter Group, Pullman, WA, USA). One sensor was installed for each clone in control treatments at 100 mm deep from the soil surface (3V-WW and A1-WW). Two sensors were installed for each clone in water stress treatments (3V-WS and A1-WS), the first at 100 mm and the second at 500 mm deep from the soil surface.

Full irrigation withholding was applied until the Ψ_{msoil} achieved the value of ca. -0.50 MPa (-500 kPa, medium to severe drought stress for coffee plants) at both soil depths (100 and 500 mm) in two water-withdrawn cycles, entitled drought-1 and drought-2 events (Figure 8). This Ψ_{msoil} was reached after 19 days of irrigation absence, after which the soil was fully rewatered until a complete recovery of A_{net} (recovery-1 and recovery-2 events). Along the experimental period, the A_{net} was measured at a PPFD of 1500 $\mu\text{mol m}^{-2} \text{s}^{-1}$ with six-day intervals. Between the drought-1 and drought-2, one period of 31 days was applied (12 days of recovery-1 followed by additional 19 days), which was considered sufficient to complete the growth of a new leaf pair [86] between the drought-1 and drought-2 events.

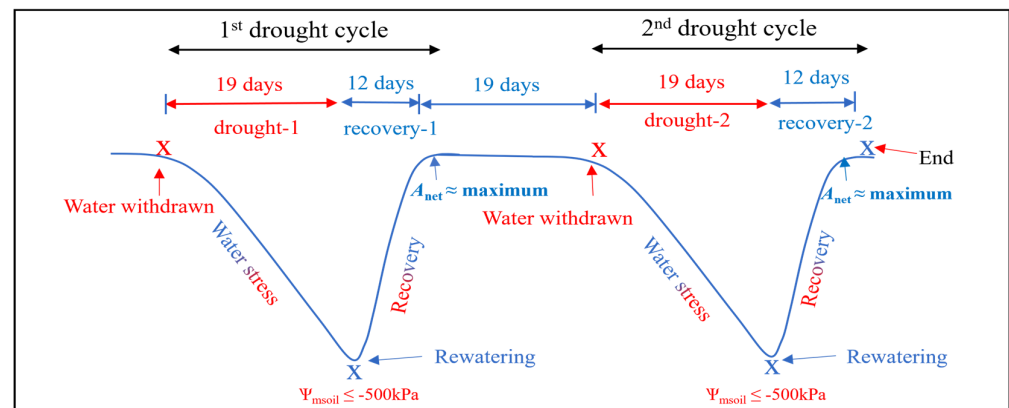


Figure 8. Diagram of the two drought cycles. Transplant followed by drought-1 event last for 19 days (until -500 kPa of Ψ_{msoil} was reached), followed by a 31-day period for a whole plant recovery (including 12-day period of recovery-1 event). The 2nd drought cycle was then applied, similarly to the 1st drought cycle, by withholding irrigation until the -500 kPa of Ψ_{msoil} was reached (drought-2 event) and followed by another 12 days of recovery-2 event.

4.2. Leaf Water Potential Measurements

Leaf water potential (Ψ_{leaf}) was measured at predawn of 20th and 68th days of experiment, at the beginning of recovery-1 and recovery-2 events, respectively, corresponding to the 1st day of rewatering. The Ψ_{leaf} measurements were made on the 3rd pair of leaves from the apex of the 3rd plagiotropic branch formed from the top of the plant ($n = 7$). This parameter was measured immediately after the leaf excision using a pressure chamber (model 3000, Soil Moisture Corp., Santa Barbara CA, USA), according to [87].

4.3. Leaf Gas Exchange Measurements

Leaf net CO_2 assimilation rate (A_{net} , $\mu\text{mol m}^{-2} \text{s}^{-1}$), stomatal conductance (g_s , $\text{mol m}^{-2} \text{s}^{-1}$), and leaf transpiration rate (E , $\text{mmol m}^{-2} \text{s}^{-1}$), together with leaf-to-air vapor pressure deficit ($\text{VPD}_{\text{leaf-air}}$, kPa), were measured using a portable open-system IRGA (Li-Cor 6400xt, LI-COR, Lincoln, NE, USA). The light source 6400-02B LED (LI-COR, Lincoln, NE, USA) was set to $1500 \mu\text{mol m}^{-2} \text{s}^{-1}$ of PPFD, and external CO_2 supply to $400 \mu\text{L L}^{-1}$. The measurements were performed at midday (between 12 a.m. and 1 p.m.) in intervals of six days in both drought events. Measurements were performed on recently fully expanded leaves, different in the 1st and 2nd drought cycles, corresponding to the 3rd or 4th leaf pair from the apex of the 2nd order plagiotropic (lateral) branches, from the upper part of the plant (about coffee architecture, see [88]). Our intention was to see if the recently fully expanded leaves would be able to respond in the next water stress event, in a time period sufficient for such development [86]. The instantaneous leaf water-use efficiency (WUE, mmol mol^{-1}) was calculated as the A_{net}/E ratio.

4.4. Chlorophyll *a* Fluorescence Evaluation

4.4.1. Non-Modulated Chlorophyll *a* Fluorescence Evaluation

Non-modulated chlorophyll (Chl) *a* fluorescence was measured in the same leaves used for the leaf gas exchange evaluations, in the same time intervals, using a Pocket PEA fluorometer (Hansatech, Norfolk, UK). The sampled leaves were dark-adapted for 30–40 min using leaf clips (same producer) to turn the reaction centers into an “open” (oxidized Q_A) state [47]. The Pocket PEA fluorometer provides the saturating light pulse of actinic light of $3500 \mu\text{mol m}^{-2} \text{s}^{-1}$. From the kinetics of fluorescence emission over time, some indices were obtained using the OJIP test, as: maximum quantum yield of primary photochemical reactions (ΦP_0); probability of electron transfer from the Q_A to electron transport chain beyond Q_A (ΨE_0); photosynthetic performance index (PI_{ABS}); and density of reaction centers capable of Q_A reduction (RC/CS_0) (Table 2).

Table 2. The evaluated indexes of non-modulated and modulated chlorophyll *a* fluorescence, plus leaf spectral indexes.

Index	Formula	Description	References
Non-Modulated Fluorescence (Pocket PEA)			
ΦP_0	$TR_0/ABS = [1 - (F_0/F_m)] = F_v/F_m$	Maximum quantum yield of primary photochemical reactions	[43,89,90]
ΨE_0	$ET_0/TR_0 = (1 - V_j)$	Probability of electron transfer from Q_A^- to electron transport chain beyond Q_A	[43,89,90]
PI_{ABS}	$(RC/ABS) \cdot [\Phi P_0 / (1 - \Phi P_0)] \cdot [\Psi_0 / (1 - \Psi_0)]$	Photosynthetic performance index	[43,89,90]
RC/CS_0	$(V_j/M_0) * (ABS/CS_0)$	Density of reaction centers capable of Q_A reduction	[43,89,90]
Modulated fluorescence (IRGA LI 6400 XT)			
Φ_{PSII}	$(F_m' - F_s)/F_m'$	Effective quantum yield in PSII photochemistry	[39,91]
qP	$(F_m' - F_s)/(F_m' - F_0')$	Photochemical quenching	[92]
NPQ	$(F_m - F_m')/F_m'$	Photo-protective process that removes excess excitation energy within chlorophyll-containing complexes and prevents the likelihood of formation of damaging free radicals. Process is considered adequate under stressful conditions if it can retain an equal fraction of open PSII reaction centers as of non-stress conditions.	[93–98]
ETR	$\Phi_{PSII} \cdot PPFD \cdot \alpha_{lea} \cdot f$	The linear electron transport rate was calculated using the photochemical efficiency at electron transport of PSII.	[99]
Reflectance indexes (CI-710)			
GCI	W_{554}/W_{677}	Green chlorophyll index	[100]
CRI	$(1/W_{510}) - (1/W_{550})$	Carotenoid reflectance index	[100]
PRI	$(W_{531} - W_{570})/(W_{531} + W_{570})$	Photochemical reflectance index	[101]
SIPI	$(W_{800} - W_{445})/(W_{800} + W_{680})$	Structure intensive pigment index	[102]

4.4.2. Modulated Chlorophyll *a* Fluorescence Evaluation

Modulated Chl *a* fluorescence was recorded using a portable photosynthesis system (LI6400XT, LI-COR, Lincoln, NE, USA) equipped with a fluorescence chamber (LI-6400-40), simultaneously as leaf gas exchange measurements, in the same time intervals, at the same leaves. The dark-adapted leaf was exposed to a weak red light ($3 \mu\text{mol m}^{-2} \text{s}^{-1}$) with a wavelength centered at 630 nm, and the leaf chamber fluorometer (LCF) detected the initial minimum fluorescence, termed F_0 . Then, after the leaf was exposed to saturation flashlights (light intensity $>7000 \mu\text{mol m}^{-2} \text{s}^{-1}$), there was an immediate rise in fluorescence to an initial maximal level, termed F_m , representing that the PSII reaction centers were completely closed and fluorescence maximized. With an actinic light provided by LCF at the intensity that was adjusted equivalent to the ambient light to drive photosynthesis ($1500 \mu\text{mol m}^{-2} \text{s}^{-1}$), the fluorescence reached a stable state on 715 nm wavelength, termed F_s . The actinic light was turned off, and a weak far-red light (the wavelength centered at about 740 nm with the intensity of $30 \mu\text{mol m}^{-2} \text{s}^{-1}$) was emitted to measure the minimal fluorescence of the light-adapted leaf, termed F_0' . An illumination of actinic light of $1500 \mu\text{mol m}^{-2} \text{s}^{-1}$ was used for a sufficient time to enable a photosynthetic steady-state condition of gas exchange parameters and photochemical dissipation. Afterwards, a saturating light pulse of $8000 \mu\text{mol m}^{-2} \text{s}^{-1}$ for 0.8 s was applied to record the light-adapted maximum fluorescence (F_m'). Immediately, the actinic light was turned off, and far-red light was applied to determine F_0' . Some indices were evaluated: Φ_{PSII} represents the effective quantum yield in PSII photochemistry; qP represents the photochemical quenching; NPQ represents the photoprotective process that removes excess excitation energy within chlorophyll-containing complexes and prevents the likelihood of formation of damaging free radicals, which is considered adequate under stressful conditions if it can retain an equal fraction of open PSII reaction centers (qP) as of non-stress conditions; and ETR represents the linear electron transport rate (Table 2).

4.5. Leaf Spectral Indices

The leaf spectral reflectance was measured on the same leaves used for the gas exchanges and fluorescence evaluations, considering the same days of the experiment period, using a CI-710/720 miniature leaf spectrometer (CID-Bioscience, Camas, WA, USA). Measurements were conducted at midday using wavelengths (W) from 400 nm to 950 nm to obtain the following calculated indices: green chlorophyll index (GCI); carotenoid reflectance index (CRI); photochemical reflectance index (PRI); and structure intensive pigment index (SIPI) (Table 2).

4.6. Leaf Anatomy

Leaf imprints from the abaxial leaf surface (from the tagged leaves used for some of the previously mentioned measurements) were taken at the end of the 2nd drought cycle and observed under a light microscope to determine stomatal density as described by [103]. Three samples of each leaf (0.050 mm² each) were observed from one field of view and averaged per plant and treatment (n = 7).

For leaf anatomical analyses of thickness of epidermis (abaxial and adaxial), palisade and spongy parenchyma, xylem vessel density, and medium vessel area, leaves were collected at the end of the 2nd drought cycle. Transverse cuts were made in the median portion of the central leaf vein. To make the cuts, leaves were stabilized in Styrofoam blocks, and the cuts were made with a razor blade. The thinnest sections were clarified with 50% sodium hypochlorite solution until they were completely translucent and washed three times in distilled water. Subsequently, they were stained with astra blue solution (1% aqueous solution) and safranin (1% alcoholic solution) in a 9:1 ratio, following methodology described by [104]. The parameters were observed with three fields of view, averaging values of each plant (n = 7) for further analyses. Photographs were taken with a Nikon Eclipse E200 optical microscope (Nikon Corp., Tokyo, Japan), using a microscope objective lens of 10× with the help of Capture 2.2.1. software (Meiji Techno, Saitama, Japan).

4.7. Statistical Analysis and Experimental Design

A completely random factorial experimental design was applied, including three factors: genotypes ('A1' and '3V'), water conditions (WW and WS), and time-points along the two drought cycles (measurements performed in six-day-frequency resulting in 12 time-points, four during each of the drought-1 and drought-2 events, and two time-points during recovery periods), except for Ψ_{leaf} , which was assessed at only one time-point per cycle, at the beginning of each of the two recovery events, while leaf anatomy was analyzed at only one time-point. All statistical analyses were performed using the 'R' programming language [105]. Three and two-way ANOVAs were processed after the use of mixed linear modeling (lme function and maximum likelihood from the 'nlme' package), considering genotypes, water availability, and time-points as fixed factor effects, while plant number (repetition) as a random effect. If no significant interaction (starting from the most complex one, where three or two factors are interacting) was found, the model reduction was applied (and fitted by using the lme function, considering again all factors as fixed or random, as mentioned before). The Bartlett homogeneity test and the Shapiro normality test were performed for each variable in each season. For comparing average values estimated by ANOVA(s), we used the Tukey HSD and 'lsmeans' and 'multcompView' packages. A significance level of 0.05 was used for all analyses. The estimated means and standard errors (SE) are shown in charts.

Supplementary Materials: The following supporting information can be downloaded at: <https://www.mdpi.com/article/10.3390/stresses4030037/s1>.

Author Contributions: Conceptualization, E.C. and D.F.B.; methodology, E.C., D.F.B. and G.A.R.d.S.; validation, all authors; formal analysis, G.A.R.d.S. and M.R.; investigation, D.F.B., G.A.R.d.S., W.d.P.B., A.R.S., L.C.d.S.B., L.F.T.B., L.Z.C., C.M.d.A. and A.C.V.F.; resources, E.C.; data curation, G.A.R.d.S., D.F.B. and M.R.; writing—original draft preparation, D.F.B. and M.R.; writing—review and editing,

M.R., W.P.R. and J.C.R.; visualization, all authors; supervision, E.C. and M.R.; project administration, E.C.; funding acquisition, E.C. All authors have read and agreed to the published version of the manuscript.

Funding: This research was funded by Fundação Carlos Chagas Filho de Amparo à Pesquisa do Estado do Rio de Janeiro (FAPERJ, Brazil) granted to E.C. (200.957/2022), together with fellowships awarded to D.F.B., W.P.B. and L.Z.C. (E-26/200.327/2020, E-26/200.172/2021, and E-26/203.158/2023). The research was additionally funded by Coordenação de Aperfeiçoamento de Pessoal de Nível Superior (CAPES, Brazil) with fellowships granted to G.A.R.S., C.M.A., A.R.S., L.C.S.B. and L.F.T.B. (88887.968322/2024-00, 88887.903335/2023-00, 88887.671147/2022-00, 88887.704841/2022-00, and 88887.822657/2023-00), by Fundação de Amparo à Pesquisa e Inovação do Espírito Santo (FAPES, Brazil) by fellowship awarded to M.R. (2022–M465D), and National Council for Scientific and Technological Development (CNPq, Brazil) by fellowship awarded to E.C. (304470/2023-6). This research was additionally funded by Fundação para a Ciência e a Tecnologia, I.P. (FCT), Portugal, through the research units CEF (UIDB/00239/2020, <https://doi.org/10.54499/UIDB/00239/2020>), and GeoBioTec (UIDP/04035/2020, <https://doi.org/10.54499/UIDB/04035/2020>), as well as through the Associate Laboratory TERRA (LA/P/0092/2020, <https://doi.org/10.54499/LA/P/0092/2020>) granted to J.C.R. The APC was funded by MDPI.

Data Availability Statement: The authors can provide experimental data for all interested researchers.

Conflicts of Interest: The authors declare no conflicts of interest.

Abbreviations

ABA: Abscisic acid; A_{net} : Leaf net CO₂ assimilation rate; Chl: Chlorophyll; CI-710/720: Miniature leaf spectrometer; CRI: Carotenoid reflectance index; E : Leaf transpiration rate; ETR: Electron transport rate; F_m : Maximum fluorescence in the dark-adapted state; F_m' : Maximum fluorescence of a light-adapted state; F_o : Minimum fluorescence in a dark-adapted state; F_o' : Minimum fluorescence of light-adapted state; F_s : Steady-state fluorescence; GCI: Leaf green chlorophyll index; Gen: Genotypes; g_m : Mesophyll conductance; g_s : Stomatal conductance; NPQ: Non-photochemical quenching; PIABS: Photosynthetic performance index; PPFD: Photosynthetic photon flux density; PRI: Photochemical reflectance index; PSII: Photosystem II; PVC: Polyvinyl chloride; qP: Photochemical quenching; RC/CS₀: Density of reaction centers capable of Q_A reduction; RH: Relative humidity; SE: Standard errors; SIPI: Structure intensive reflectance index; T_{air} : Air temperature; VPD_{air}: Air vapor pressure deficit; VPD_{leaf-air}: Leaf-to-air vapor pressure deficit; WS: Water stressed; WUE (A_{net}/E): Instantaneous water-use efficiency; WW: Well-watered; ΦP_0 : Maximum quantum yield of primary photochemical reactions; Φ_{PSII} : Effective quantum yield in PSII photochemistry; ΨE_0 : Probability of electron transfer from Q_A⁻ to electron transport chain beyond Q_A; Ψ_{leaf} : Leaf water potential; Ψ_{msoil} : Soil matric water potential.

References

1. Davis, A.P.; Rakotonasolo, F. Six new species of coffee (*Coffea*) from northern Madagascar. *Kew Bull.* **2021**, *76*, 497–511. [[CrossRef](#)]
2. DaMatta, F.M.; Avila, R.T.; Cardoso, A.A.; Martins, S.C.V.; Ramalho, J.C. Physiological and agronomic performance of the coffee crop in the context of climate change and global warming: A review. *J. Agric. Food Chem.* **2018**, *66*, 5264–5274. [[CrossRef](#)] [[PubMed](#)]
3. Filho, J.A.M.; Rodrigues, W.P.; Baroni, D.F.; Pireda, S.; Campbell, G.; de Souza, G.A.R.; Filho, A.C.V.; Arantes, S.D.; Arantes, L.d.O.; da Cunha, M.; et al. Linking root and stem hydraulic traits to leaf physiological parameters in *Coffea canephora* clones with contrasting drought tolerance. *J. Plant Physiol.* **2021**, *258*, 153355. [[CrossRef](#)]
4. CONAB. Clima Mais Favorável e Bionalidade Positiva Apontam Produção Estimada em 58,08 milhões de Sacas de Café. 2024. Available online: <https://www.conab.gov.br/ultimas-noticias/5362-clima-mais-favoravel-e-bionalidade-positiva-apontam-producao-estimada-em-58-08-milhoes-de-sacas-de-cafe> (accessed on 25 July 2024).
5. Venancio, L.P.; Filgueiras, R.; Mantovani, E.C.; Amaral, C.H.D.; da Cunha, F.F.; Silva, F.C.d.S.; Althoff, D.; dos Santos, R.A.; Cavatte, P.C. Impact of drought associated with high temperatures on *Coffea canephora* plantations: A case study in Espírito Santo State, Brazil. *Sci. Rep.* **2020**, *10*, 1–21. [[CrossRef](#)] [[PubMed](#)]
6. Ingraio, C.; Strippoli, R.; Lagioia, G.; Huisingh, D. Water scarcity in agriculture: An overview of causes, impacts and approaches for reducing the risks. *Heliyon* **2023**, *9*, e18507. [[CrossRef](#)]

7. DaMatta, F.M.; Grandis, A.; Arenque, B.C.; Buckeridge, M.S. Impacts of climate changes on crop physiology and food quality. *Food Res. Int.* **2010**, *43*, 1814–1823. [[CrossRef](#)]
8. Silva, P.E.M.; Cavatte, P.C.; Morais, L.E.; Medina, E.F.; DaMatta, F.M. The functional divergence of biomass partitioning, carbon gain and water use in *Coffea canephora* in response to the water supply: Implications for breeding aimed at improving drought tolerance. *Environ. Exp. Bot.* **2013**, *87*, 49–57. [[CrossRef](#)]
9. Fang, Y.; Xiong, L. General mechanisms of drought response and their application in drought resistance improvement in plants. *Cell. Mol. Life Sci.* **2015**, *72*, 673–689. [[CrossRef](#)]
10. Manavalan, L.P.; Guttikonda, S.K.; Tran, L.S.; Nguyen, H.T. Physiological and molecular approaches to improve drought resistance in soybean. *Plant Cell Physiol.* **2009**, *50*, 1260–1276. [[CrossRef](#)] [[PubMed](#)]
11. Yue, B.; Xue, W.; Xiong, L.; Yu, X.; Luo, L.; Cui, K.; Jin, D.; Xing, Y.; Zhang, Q. Genetic basis of drought resistance at reproductive stage in rice: Separation of drought tolerance from drought avoidance. *Genetics* **2006**, *172*, 1213–1228. [[CrossRef](#)]
12. Tardieu, F. Plant response to environmental conditions: Assessing potential production, water demand, and negative effects of water deficit. *Front. Physiol.* **2013**, *4*, 35373. [[CrossRef](#)]
13. Siddique, K.H.M.; Belford, R.K.; Tennant, D. Root: Shoot ratios of old and modern, tall and semi-dwarf wheats in a mediterranean environment. *Plant Soil* **1990**, *121*, 89–98. [[CrossRef](#)]
14. Hammer, G.L.; Dong, Z.; McLean, G.; Doherty, A.; Messina, C.; Schussler, J.; Zinselmeier, C.; Paszkiewicz, S.; Cooper, M. Can changes in canopy and/or root system architecture explain historical maize yield trends in the US corn belt? *Crop Sci.* **2009**, *49*, 299–312. [[CrossRef](#)]
15. Steele, K.A.; Price, A.H.; Witcombe, J.R.; Shrestha, R.; Singh, B.N.; Gibbons, J.M.; Virk, D.S. QTLs associated with root traits increase yield in upland rice when transferred through marker-assisted selection. *Theor. Appl. Genet.* **2012**, *126*, 101–108. [[CrossRef](#)] [[PubMed](#)]
16. De Lima, V.J.; Júnior, A.T.D.A.; Kamphorst, S.H.; Bispo, R.B.; Leite, J.T.; Santos, T.d.O.; Schmitt, K.F.M.; Chaves, M.M.; de Oliveira, U.A.; Santos, P.H.A.D.; et al. Combined dominance and additive gene effects in trait inheritance of drought-stressed and full irrigated popcorn. *Agronomy* **2019**, *9*, 782. [[CrossRef](#)]
17. Gambetta, G.A.; Knipfer, T.; Fricke, W.; McElrone, A.J. Aquaporins and root water uptake. In *Plant Aquaporins. from Signaling and Communication in Plants*; Chaumont, F., Tyerman, S.D., Eds.; Springer International Publishing: New York, NY, USA, 2017; Volume 10, pp. 133–153.
18. Chen, D.; Wang, S.; Cao, B.; Cao, D.; Leng, G.; Li, H.; Yin, L.; Shan, L.; Deng, X. Genotypic variation in growth and physiological response to drought stress and re-watering reveals the critical role of recovery in drought adaptation in maize seedlings. *Front. Plant Sci.* **2016**, *6*, 1241. [[CrossRef](#)]
19. Ramalho, J.; Chaves, M.M. Drought effects on plant water relations and carbon gain in two lines of *Lupinus albus* L. *Eur. J. Agron.* **1992**, *1*, 271–280. [[CrossRef](#)]
20. Ennajeh, M.; Vadel, A.M.; Cochard, H.; Khemira, H. Comparative impacts of water stress on the leaf anatomy of a drought-resistant and a drought-sensitive olive cultivar. *J. Hortic. Sci. Biotechnol.* **2010**, *85*, 289–294. [[CrossRef](#)]
21. Martins, S.C.V.; Sanglard, M.L.; Morais, L.E.; Menezes-Silva, P.E.; Mauri, R.; Avila, R.T.; Vital, C.E.; Cardoso, A.A.; DaMatta, F.M. How do coffee trees deal with severe natural droughts? An analysis of hydraulic, diffusive and biochemical components at the leaf level. *Trees* **2019**, *33*, 1679–1693. [[CrossRef](#)]
22. Fernandes, I.; Marques, I.; Paulo, O.S.; Batista, D.; Partelli, F.L.; Lidon, F.C.; DaMatta, F.M.; Ramalho, J.C.; Ribeiro-Barros, A.I. Understanding the impact of drought in *Coffea* genotypes: Transcriptomic analysis supports a common high resilience to moderate water deficit but a genotype dependent sensitivity to severe water deficit. *Agronomy* **2021**, *11*, 2255. [[CrossRef](#)]
23. DaMatta, F.M.; Rahn, E.; Läderach, P.; Ghini, R.; Ramalho, J.C. Why could the coffee crop endure climate change and global warming to a greater extent than previously estimated? *Clim. Change* **2019**, *152*, 167–178. [[CrossRef](#)]
24. Martins, S.C.V.; Galmés, J.; Cavatte, P.C.; Pereira, L.F.; Ventrella, M.C.; DaMatta, F.M. Understanding the low photosynthetic rates of sun and shade coffee leaves: Bridging the gap on the relative roles of hydraulic, diffusive and biochemical constraints to photosynthesis. *PLoS ONE* **2014**, *9*, e95571. [[CrossRef](#)]
25. Peloso, A.F.; Tatagiba, S.D.; Reis, E.F.; Pezzopane, J.E.M.; Amaral, F.F.T. Photosynthetic limitations in leaves of Arabic coffee promoted by the water deficit. *Coffee Sci.* **2017**, *12*, 389–399. [[CrossRef](#)]
26. Smedo, J.N.; Rodrigues, A.P.; Lidon, F.C.; Pais, I.P.; Marques, I.; Gouveia, D.; Armengaud, J.; Silva, M.J.; Martins, S.; Smedo, M.C.; et al. Intrinsic non-stomatal resilience to drought of the photosynthetic apparatus in *Coffea* spp. is strengthened by elevated air [CO₂]. *Tree Physiol.* **2021**, *41*, 708–727. [[CrossRef](#)] [[PubMed](#)]
27. Da Silva, P.C.; Junior, W.Q.R.; Ramos, M.L.G.; Rocha, O.C.; Veiga, A.D.; Silva, N.H.; Brasileiro, L.d.O.; Santana, C.C.; Soares, G.F.; Malaquias, J.V.; et al. Physiological changes of arabica coffee under different intensities and durations of water stress in the Brazilian Cerrado. *Plants* **2022**, *11*, 2198. [[CrossRef](#)] [[PubMed](#)]
28. Melo, E.F.; Fernandes-Brum, C.N.; Pereira, F.J.; de Castro, E.M.; Chalfun-Júnior, A. Anatomic and physiological modifications in seedlings of *Coffea arabica* cultivar Siriema under drought conditions. *Cienc. Agrotec.* **2014**, *38*, 25–33. [[CrossRef](#)]
29. Rodrigues, A.P.; Pais, I.P.; Leitão, A.E.; Dubberstein, D.; Lidon, F.C.; Marques, I.; Smedo, J.N.; Rakocevic, M.; Scotti-Campos, P.; Campostrini, E.; et al. Uncovering the wide protective responses in *Coffea* spp. leaves to single and superimposed exposure of warming and severe water deficit. *Front. Plant Sci.* **2024**, *14*, 1320552. [[CrossRef](#)]

30. Beyel, V.; Bruggemann, W. Differential inhibition of photosynthesis during pre-flowering drought stress in *Sorghum bicolor* genotypes with different senescence traits. *Physiol. Plant.* **2005**, *124*, 249–259. [[CrossRef](#)]
31. Xu, Z.Z.; Zhou, G.S.; Wang, Y.L.; Han, G.X.; Li, Y.J. Changes in chlorophyll fluorescence in maize plants with imposed rapid de-hydration at different leaf ages. *J. Plant Growth Regul.* **2008**, *27*, 83–92. [[CrossRef](#)]
32. Guóth, A.; Tari, I.; Gallé, A.; Csiszár, J.; Pécsváradi, A.; Cseuz, L.; Erdei, L. Comparison of the drought stress responses of tolerant and sensitive wheat cultivars during grain filling: Changes in flag leaf photosynthetic activity, ABA levels, and grain yield. *J. Plant Growth Regul.* **2009**, *28*, 167–176. [[CrossRef](#)]
33. Ramalho, J.C.; Rodrigues, A.P.; Lidon, F.C.; Marques, L.M.C.; Leitão, A.E.; Fortunato, A.S.; Pais, I.P.; Silva, M.J.; Scotti-Campos, P.; Lopes, A.; et al. Stress cross-response of the antioxidative system promoted by superimposed drought and cold conditions in *Coffea* spp. *PLoS ONE* **2018**, *13*, e0198694. [[CrossRef](#)] [[PubMed](#)]
34. Scotti-Campos, P.; Pais, I.P.; Ribeiro-Barros, A.I.; Martins, L.D.; Tomaz, M.A.; Rodrigues, W.P.; Campostrini, E.; Smedo, J.N.; Fortunato, A.S.; Martins, M.Q.; et al. Lipid profile adjustments may contribute to warming acclimation and to heat impact mitigation by elevated [CO₂] in *Coffea* spp. *Environ. Exp. Bot.* **2019**, *167*, 103856. [[CrossRef](#)]
35. Rodrigues, A.M.; Jorge, T.; Osorio, S.; Pott, D.M.; Lidon, F.C.; DaMatta, F.M.; Marques, I.; Ribeiro-Barros, A.I.; Ramalho, J.C.; António, C. Primary metabolite profile changes in *Coffea* spp. promoted by single and combined exposure to drought and elevated CO₂ concentration. *Metabolites* **2021**, *11*, 427. [[CrossRef](#)]
36. Marques, I.; Gouveia, D.; Gaillard, J.-C.; Martins, S.; Smedo, M.C.; Lidon, F.C.; DaMatta, F.M.; Ribeiro-Barros, A.I.; Armengaud, J.; Ramalho, J.C. Next-generation proteomics reveals a greater antioxidative response to drought in *Coffea arabica* than in *Coffea canephora*. *Agronomy* **2022**, *12*, 148. [[CrossRef](#)]
37. Driesen, E.; de Proft, M.; Saeys, W. Drought stress triggers alterations of adaxial and abaxial stomatal development in basil leaves increasing water-use efficiency. *Hortic. Res.* **2023**, *10*, uhad075. [[CrossRef](#)] [[PubMed](#)]
38. Ripoll, J.; Bertin, N.; Bidet, L.P.R.; Urban, L. A user's view of the parameters derived from the induction curves of maximal chlorophyll *a* fluorescence: Perspectives for analyzing stress. *Front. Plant Sci.* **2016**, *7*, 1679. [[CrossRef](#)]
39. Rodrigues, W.P.; Martins, M.Q.; Fortunato, A.S.; Rodrigues, A.P.; Smedo, J.N.; Simões-Costa, M.C.; Pais, I.P.; Leitão, A.E.; Colwell, F.; Goulao, L.; et al. Long-term elevated air [CO₂] strengthens photosynthetic functioning and mitigates the impact of supra-optimal temperatures in tropical *Coffea arabica* and *C. canephora* species. *Glob. Change Biol.* **2016**, *22*, 415–431. [[CrossRef](#)]
40. Misra, A.N.; Misra, M.; Singh, R. Chlorophyll fluorescence in plant biology. In *Biophysics*; Misra, A.N., Ed.; Intech: Shanghai, China, 2012; Volume 7, pp. 171–192.
41. Kalaji, H.M.; Jajoo, A.; Oukarroum, A.; Brestic, M.; Zivcak, M.; Samborska, I.A.; Cetner, M.D.; Łukasik, I.; Goltsev, V.; Ladle, R.J. Chlorophyll *a* fluorescence as a tool to monitor physiological status of plants under abiotic stress conditions. *Acta Physiol. Plant.* **2016**, *38*, 1–11. [[CrossRef](#)]
42. Kalaji, H.M.; Schansker, G.; Ladle, R.J.; Goltsev, V.; Bosa, K.; Allakhverdiev, S.I.; Brestic, M.; Bussotti, F.; Calatayud, A.; Dąbrowski, P.; et al. Frequently asked questions about in vivo chlorophyll fluorescence: Practical issues. *Photosynth. Res.* **2014**, *122*, 121–158. [[CrossRef](#)]
43. Strasser, R.J.; Srivastava, A.; Govindjee. Polyphasic chlorophyll *a* fluorescence transient in plants and cyanobacteria. *Photochem. Photobiol.* **1995**, *61*, 32–42. [[CrossRef](#)]
44. Yin, Z.; Meng, F.; Song, H.; He, X.; Xu, X.; Yu, D. Mapping quantitative trait loci associated with chlorophyll *a* fluorescence parameters in soybean (*Glycine max* (L.) Merr.). *Planta* **2010**, *231*, 875–885. [[CrossRef](#)] [[PubMed](#)]
45. Rodrigues, W.P.; Vieira, H.D.; Campostrini, E.; Figueiredo, F.A.M.M.A.; Ferraz, T.M.; Partelli, F.L.; Ramalho, J.C. Physiological aspects, growth and yield of *Coffea* spp. in areas of high altitude. *Aust. J. Crop Sci.* **2016**, *10*, 666–674. [[CrossRef](#)]
46. Van Kooten, O.; Snel, J.F. The use of chlorophyll fluorescence nomenclature in plant stress physiology. *Photosynth. Res.* **1990**, *25*, 147–150. [[CrossRef](#)]
47. Bolhar-Nordenkamp, H.R.; Long, S.P.; Baker, N.R.; Oquist, G.; Schreiber, U.; Lechner, E.G. Chlorophyll fluorescence as a probe of the photosynthetic competence of leaves in the field: A review of current instrumentation. *Funct. Ecol.* **1989**, *3*, 497–514. [[CrossRef](#)]
48. Martins, M.Q.; Rodrigues, W.P.; Fortunato, A.S.; Leitão, A.E.; Rodrigues, A.P.; Pais, I.P.; Martins, L.D.; Silva, M.J.; Reboredo, F.H.; Partelli, F.L.; et al. Protective response mechanisms to heat stress in interaction with high [CO₂] conditions in *Coffea* spp. *Front. Plant Sci.* **2016**, *7*, 947. [[CrossRef](#)] [[PubMed](#)]
49. Dubberstein, D.; Lidon, F.C.; Rodrigues, A.P.; Smedo, J.N.; Marques, I.; Rodrigues, W.P.; Gouveia, D.; Armengaud, J.; Smedo, M.C.; Martins, S.; et al. Resilient and sensitive key points of the photosynthetic machinery of *Coffea* spp. to the single and superimposed exposure to severe drought and heat stresses. *Front. Plant Sci.* **2020**, *11*, 1049. [[CrossRef](#)] [[PubMed](#)]
50. Sukhova, E.; Yudina, L.; Gromova, E.; Ryabkova, A.; Vodeneev, V.; Sukhov, V. Influence of local burning on difference reflectance indices based on 400–700 nm wavelengths in leaves of pea seedlings. *Plants* **2021**, *10*, 878. [[CrossRef](#)]
51. Sun, P.; Grignetti, A.; Liu, S.; Casacchia, R.; Salvatori, R.; Pietrini, F.; Loreto, F.; Centritto, M. Associated changes in physiological parameters and spectral reflectance indices in olive (*Olea europaea* L.) leaves in response to different levels of water stress. *Int. J. Remote Sens.* **2008**, *29*, 1725–1743. [[CrossRef](#)]
52. Kior, A.; Sukhov, V.; Sukhova, E. Application of reflectance indices for remote sensing of plants and revealing actions of stressors. *Photonics* **2021**, *8*, 582. [[CrossRef](#)]

53. Menezes-Silva, P.E.; Sanglard, L.M.; Ávila, R.T.; Morais, L.E.; Martins, S.C.; Nobres, P.; Patreze, C.M.; Ferreira, M.A.; Araújo, W.L.; Fernie, A.R.; et al. Photosynthetic and metabolic acclimation to repeated drought events play key roles in drought tolerance in coffee. *J. Exp. Bot.* **2017**, *68*, 4309–4322. [[CrossRef](#)]
54. Marques, I.; Fernandes, I.; Paulo, O.S.; Batista, D.; Lidon, F.C.; Rodrigues, A.P.; Partelli, F.L.; DaMatta, F.M.; Ribeiro-Barros, A.I.; Ramalho, J.C. Transcriptomic analyses reveal that *Coffea arabica* and *Coffea canephora* have more complex responses under combined heat and drought than under individual stressors. *Int. J. Mol. Sci.* **2024**, *25*, 7995. [[CrossRef](#)]
55. Galle, A.; Florez-Sarasa, I.; El Aououad, H.; Flexas, J. The Mediterranean evergreen *Quercus ilex* and the semi-deciduous *Cistus albidus* differ in their leaf gas exchange regulation and acclimation to repeated drought and re-watering cycles. *J. Exp. Bot.* **2011**, *62*, 5207–5216. [[CrossRef](#)] [[PubMed](#)]
56. Rakočević, M.; Costes, E.; Campostrini, E.; Ramalho, J.C.; Ribeiro, R.V. Drought responses in *Coffea arabica* as affected by genotype and phenophase. II—Photosynthesis at leaf and plant scales. *Exp. Agric.* **2024**, *60*, e7. [[CrossRef](#)]
57. Perrone, I.; Pagliarani, C.; Lovisolò, C.; Chitarra, W.; Roman, F.; Schubert, A. Recovery from water stress affects grape leaf petiole transcriptome. *Planta* **2012**, *235*, 1383–1396. [[CrossRef](#)] [[PubMed](#)]
58. Bruce, T.J.A.; Matthes, M.C.; Napier, J.A.; Pickett, J.A. Stressful ‘memories’ of plants: Evidence and possible mechanisms. *Plant Sci.* **2007**, *173*, 603–608. [[CrossRef](#)]
59. Iwasaki, M.; Paszkowski, J. Epigenetic memory in plants. *EMBO J.* **2014**, *33*, 1–12. [[CrossRef](#)]
60. Fleta-Soriano, E.; Munné-Bosch, S. Stress memory and the inevitable effects of drought: A physiological perspective. *Front. Plant Sci.* **2016**, *7*, 143. [[CrossRef](#)]
61. Rakočević, M.; Matsunaga, F.T.; Pazianotto, R.A.A.; Ramalho, J.C.; Costes, E.; Ribeiro, R.V. Drought responses in *Coffea arabica* as affected by genotype and phenophase. I—Leaf distribution and branching. *Exp. Agric.* **2024**, *60*, e7. [[CrossRef](#)]
62. Tyree, M.T.; Sperry, J.S. Do woody plants operate near the point of catastrophic xylem dysfunction caused by dynamic water stress? Answers from a model. *Plant Physiol.* **1988**, *88*, 574–580. [[CrossRef](#)]
63. Sperry, J.S.; Adler, F.R.; Campbell, G.S.; Comstock, J.P. Limitation of plant water use by rhizosphere and xylem conductance: Results from a model. *Plant Cell Environ.* **1998**, *21*, 347–359. [[CrossRef](#)]
64. Whitehead, D. Regulation of stomatal conductance and transpiration in forest canopies. *Tree Physiol.* **1998**, *18*, 633–644. [[CrossRef](#)] [[PubMed](#)]
65. McDowell, N.; Pockman, W.T.; Allen, C.D.; Breshears, D.D.; Cobb, N.; Kolb, T.; Plaut, J.; Sperry, J.; West, A.; Williams, D.G.; et al. Mechanisms of plant survival and mortality during drought: Why do some plants survive while others succumb to drought? *New Phytol.* **2008**, *178*, 719–739. [[CrossRef](#)] [[PubMed](#)]
66. Zhang, L.; Niu, Y.; Zhang, H.; Han, W.; Li, G.; Tang, J.; Peng, X. Maize canopy temperature extracted from UAV thermal and RGB imagery and its application in water stress monitoring. *Front. Plant Sci.* **2019**, *10*, 1270. [[CrossRef](#)] [[PubMed](#)]
67. Flexas, J.; Ribas-Carbo, M.; Bota, J.; Galmés, J.; Henkle, M.; Martínez-Canellas, S.; Medrano, H. Decreased Rubisco activity during water stress is not induced by decreased relative water content but related to conditions of low stomatal conductance and chloroplast CO₂ concentration. *New Phytol.* **2006**, *172*, 73–82. [[CrossRef](#)]
68. Aliche, E.B.; Prusova-Bourke, A.; Ruiz-Sanchez, M.; Oortwijn, M.; Gerkema, E.; van As, H.; Visser, R.G.F.; van der Linden, C.G. Morphological and physiological responses of the potato stem transport tissues to dehydration stress. *Planta* **2020**, *251*, 45. [[CrossRef](#)]
69. Aro, E.-M.; Virgin, I.; Andersson, B. Photoinhibition of photosystem II. Inactivation, protein damage and turnover. *Biochim. Biophys. Acta Bioenerg.* **1993**, *1143*, 113–134. [[CrossRef](#)]
70. Fantuzzi, A.; Allgöwer, F.; Baker, H.; McGuire, G.; Te, W.K.; Gamiz-Hernandez, A.P.; Kaila, V.R.I.; Rutherford, A.W. Bicarbonate-controlled reduction of oxygen by the QA semiquinone in photosystem II in membranes. *Proc. Natl. Acad. Sci. USA* **2022**, *119*, e2116063119. [[CrossRef](#)]
71. Guidi, L.; Lo Piccolo, E.; Landi, M. Chlorophyll fluorescence, photoinhibition and abiotic stress: Does it make any difference the fact to be a C3 or C4 species? *Front. Plant Sci.* **2019**, *10*, 174. [[CrossRef](#)]
72. Demmig-Adams, B.; Koh, S.C.; Cohu, C.; Muller, O.; Stewart, J.; Adams, W., III. Non-photochemical fluorescence quenching in contrasting plant species and environments. In *Non-Photochemical Quenching and Energy Dissipation in Plants, Algae and Cyanobacteria*; Demmig-Adams, B., Garab, G., Adams, W., III, Eds.; Springer: Dordrecht, The Netherlands, 2014; Volume 40, pp. 531–552.
73. Nakamura, Y.; Tsujimoto, K.; Ogawa, T.; Noda, H.M.; Hikosaka, K. Correction of photochemical reflectance index (PRI) by optical indices to predict non-photochemical quenching (NPQ) across various species. *Remote Sens. Environ.* **2024**, *305*, 114062. [[CrossRef](#)]
74. Muller-Moulé, P.; Conklin, P.L.; Niyogi, K.K. Ascorbate deficiency can limit violaxanthin de-epoxidase activity in vivo. *Plant Physiol.* **2002**, *128*, 970–977. [[CrossRef](#)]
75. Chen, X.; Li, W.; Lu, Q.; Wen, X.; Li, H.; Kuang, T.; Li, Z.; Lu, C. The xanthophyll cycle and antioxidative defense system are enhanced in the wheat hybrid subjected to high light stress. *J. Plant Physiol.* **2011**, *167*, 1828–1836. [[CrossRef](#)] [[PubMed](#)]
76. Niu, Y.; Wang, Y.; Li, P.; Zhang, F.; Liu, H.; Zheng, G. Drought stress induces oxidative stress and the antioxidant defense system in ascorbate-deficient vtc1 mutants of *Arabidopsis thaliana*. *Acta Physiol. Plant.* **2013**, *35*, 1189–1200. [[CrossRef](#)]

77. Quinlan, R.F.; Shumskaya, M.; Bradbury, L.M.; Beltrán, J.; Ma, C.; Kennelly, E.J.; Wurtzel, E.T. Synergistic interactions between carotene ring hydroxylases drive lutein formation in plant carotenoid biosynthesis. *Plant Physiol.* **2012**, *160*, 204–214. [[CrossRef](#)] [[PubMed](#)]
78. Sudrajat, D.J.; Siregar, I.Z.; Khumaida, N.; Siregar, U.J.; Mansur, I. Adaptability of white jabon (*Anthocephalus cadamba* MIQ.) seedling from 12 populations to drought and waterlogging. *Agrivita J. Agric. Sci.* **2015**, *37*, 130–143. [[CrossRef](#)]
79. DaMatta, F.M.; Chaves, A.R.; Pinheiro, H.A.; Ducatti, C.; Loureiro, M.E. Drought tolerance of two field-grown clones of *Coffea canephora*. *Plant Sci.* **2003**, *164*, 111–117. [[CrossRef](#)]
80. Pinheiro, H.A.; DaMatta, F.M.; Chaves, A.R.M.; Loureiro, M.E.; Ducatti, C. Drought tolerance is associated with rooting depth and stomatal control of water use in clones of *Coffea canephora*. *Ann. Bot.* **2005**, *96*, 101–108. [[CrossRef](#)]
81. Reddy, K.S.; Sekhar, K.M.; Sreeharsha, R.V.; Reddy, A.R. Hydraulic dynamics and photosynthetic performance facilitate rapid screening of field grown mulberry (*Morus* spp.) genotypes for drought tolerance. *Environ. Exp. Bot.* **2019**, *157*, 320–330. [[CrossRef](#)]
82. Nteve, G.-M.; Kostas, S.; Polidoros, A.N.; Madesis, P.; Nianiou-Obeidat, I. Adaptation mechanisms of olive tree under drought stress: The potential of modern omics approaches. *Agriculture* **2024**, *14*, 579. [[CrossRef](#)]
83. Guedes, F.A.d.F.; Nobres, P.; Ferreira, D.C.R.; Menezes-Silva, P.E.; Ribeiro-Alves, M.; Correa, R.L.; DaMatta, F.M.; Alves-Ferreira, M. Transcriptional memory contributes to drought tolerance in coffee (*Coffea canephora*) plants. *Environ. Exp. Bot.* **2018**, *147*, 220–233. [[CrossRef](#)]
84. Rakočević, M.; Baroni, D.F.; de Souza, G.A.R.; Bernado, W.P.; Almeida, C.M.; Matsunaga, F.T.; Rodrigues, W.P.; Ramalho, J.C.; Campostrini, E. Correlating *Coffea canephora* 3D architecture to plant photosynthesis at a daily scale and vegetative biomass allocation. *Tree Physiol.* **2023**, *43*, 556–574. [[CrossRef](#)]
85. Sousa, J.S.; Neves, J.C.L.; Martinez, H.E.P.; Alvarez, V.H.V. Relationship between coffee leaf analysis and soil chemical analysis. *Rev. Bras. Cienc. Solo* **2018**, *42*, e0170109. [[CrossRef](#)]
86. Rakočević, M.; Matsunaga, F.T. Variations in leaf growth parameters within the tree structure of adult *Coffea arabica* in relation to seasonal growth, water availability and air carbon dioxide concentration. *Ann. Bot.* **2018**, *122*, 117–131. [[CrossRef](#)] [[PubMed](#)]
87. Schölander, P.F.; Bradstreet, E.D.; Hemmingen, E.A.; Hammel, H.T. Sap pressure in vascular plants: Negative hydrostatic pressure can be measured in plants. *Science* **1965**, *148*, 339–346. [[CrossRef](#)] [[PubMed](#)]
88. Rakočević, M. Coffee plant architecture. Advances in Botanical Research. In *Coffee—A Glimpse into the Future*, 114th ed.; DaMatta, F.M., Ramalho, J.C., Eds.; Elsevier: Amsterdam, The Netherlands, 2024. [[CrossRef](#)] [[PubMed](#)]
89. Strasser, R.J.; Tsimilli-Michael, M. Stress in plants, from daily rhythm to global changes, detected and quantified by the JIP-test. *Chim. Novv.* **2001**, *75*, 3321–3326.
90. Strasser, R.J.; Srivastava, A.; Tsimilli-Michael, M.; Srivastava, A. Analysis of the chlorophyll a fluorescence transient. In *Advances in Photosynthesis and Respiration*; Sharkey, T.D., Eaton-Rye, J.J., Eds.; Kluwer Academic Publishers: Dordrecht, The Netherlands, 2004; Volume 19, pp. 321–362.
91. Genty, B.; Briantais, J.M.; Baker, N.R. The relation between the quantum yield of photosynthetic electron transport and quenching of chlorophyll fluorescence. *Biochim. Biophys. Acta* **1989**, *990*, 87–92. [[CrossRef](#)]
92. Murchie, E.H.; Lawson, T. Chlorophyll fluorescence analysis: A guide to good practice and understanding some new applications. *J. Exp. Bot.* **2013**, *64*, 3983–3998. [[CrossRef](#)] [[PubMed](#)]
93. Krall, J.; Edwards, G. Environmental effects on the relationship between the quantum yields of carbon assimilation and in vivo PSII electron transport in maize. *Funct. Plant Biol.* **1991**, *18*, 267–278. [[CrossRef](#)]
94. Lambrev, P.H.; Miloslavina, Y.; Jahns, P.; Holzwarth, A.R. On the relationship between non-photochemical quenching and photo-protection of photosystem II. *Biochim Biophys Acta.* **2012**, *1817*, 760–769. [[CrossRef](#)]
95. Foyer, C.H.; Ruban, A.V.; Noctor, G. Viewing oxidative stress through the lens of oxidative signalling rather than damage. *Biochem. J.* **2017**, *474*, 877–883. [[CrossRef](#)]
96. Foyer, C.H. Reactive oxygen species, oxidative signaling and the regulation of photosynthesis. *Environ. Exp. Bot.* **2018**, *154*, 134–142. [[CrossRef](#)]
97. Czarnocka, W.; Karpiński, S. Friend or foe? Reactive oxygen species production, scavenging and signaling in plant response to environmental stresses. *Free. Radic. Biol. Med.* **2018**, *122*, 4–20. [[CrossRef](#)] [[PubMed](#)]
98. Moustakas, M. Plant photochemistry, reactive oxygen species, and photoprotection. *Photochem* **2022**, *2*, 5–8. [[CrossRef](#)]
99. Baker, N.R. Chlorophyll fluorescence: A probe of photosynthesis In Vivo. *Annu. Rev. Plant Biol.* **2008**, *59*, 89–113. [[CrossRef](#)] [[PubMed](#)]
100. Gitelson, A.A.; Zur, Y.; Chivkunova, O.B.; Merzlyak, M.N. Assessing carotenoid content in plant leaves with reflectance spectroscopy. *Photochem. Photobiol.* **2007**, *75*, 272–281. [[CrossRef](#)]
101. Gamon, J.A.; Serrano, L.; Surfus, J.S. The photochemical reflectance index: An optical indicator of photosynthetic radiation use efficiency across species, functional types, and nutrient levels. *Oecologia* **1997**, *112*, 492–501. [[CrossRef](#)]
102. Peñuelas, J.; Baret, F.; Filella, I. Semi-empirical indices to assess carotenoids/chlorophyll-a ratio from leaf spectral reflectance. *Pho-tosynthetic* **1995**, *31*, 221–230.
103. Ramalho, J.C.; Rodrigues, A.P.; Smedo, J.N.; Pais, I.P.; Martins, L.D.; Simões-Costa, M.C.; Leitão, A.E.; Fortunato, A.S.; Batista-Santos, P.; Palos, I.M.; et al. Sustained Photosynthetic Performance of *Coffea* spp. under Long-Term Enhanced [CO₂]. *PLoS ONE* **2013**, *8*, e82712. [[CrossRef](#)]

-
104. Neto, B.C.; Silva, F.; Ferreira, T.; Crasque, J.; Arantes, L.; Filho, J.M.; DE Souza, T.; Falqueto, A.; Dousseau-Arantes, S. Responses of wild Piper species to drought and rehydration cycles considering stomatal closure as a marker of the alarm phase. *Photosynthetica* **2023**, *61*, 363–376. [[CrossRef](#)]
 105. R Core Team. Available online: <https://www.r-project.org/> (accessed on 14 April 2024).

Disclaimer/Publisher’s Note: The statements, opinions and data contained in all publications are solely those of the individual author(s) and contributor(s) and not of MDPI and/or the editor(s). MDPI and/or the editor(s) disclaim responsibility for any injury to people or property resulting from any ideas, methods, instructions or products referred to in the content.